2015

DEPARTAMENTO DE CIÊNCIAS DA VIDA

FACULDADE DE CIÊNCIAS E TECNOLOGIA

UNIVERSIDADE DE COIMBRA

Role of Shisa6 on AMPAR surface mobility and nano-organization

Tiago Miguel Sá Campelo

2015

Role of Shisa6 on AMPAR surface mobility and nano-organization

Tiago Miguel Sá Campelo

DEPARTAMENTO DE CIÊNCIAS DA VIDA

FACULDADE DE CIÊNCIAS E TECNOLOGIA

UNIVERSIDADE DE COIMBRA

Role of Shisa6 on AMPAR surface mobility and nano-organization

Papel da Shisa6 na regulação da mobilidade e nano-organização dos receptores AMPA

Dissertação apresentada à Universidade de Coimbra para cumprimento dos requesitos necessários à obtenção do grau de Mestre em Biologia Molecular e Celular, realizada sob a orientação científica da Doutora Françoise Coussen (Universidade de Bordéus, França) e da Professora Doutora Ana Luisa Carvalho (Universidade de Coimbra).

Tiago Miguel Sá Campelo

2015

The work hereby presented was performed at the Institute Interdisciplinary for Neuroscience – IINS, Bordeaux, France and funded by European Research Council "grant ADOS to Doctor Daniel Choquet", the Agence Natonale de la Recherche, the Aquitaine region, and "Acção Integrada Luso-Francesa FP 01/13".

Acknowledgments

I would first and foremost like to thank Dr. Daniel Choquet, director of the IINS and "Dynamics of Synapse Organization" team, for having welcomed me into his laboratory and his team for my Master thesis internship.

I would like to especially thank both my internship supervisors, Françoise Coussen and Eric Hosy, for being incredible patient, helpful and insightful throughout the duration of my internship. I wish also to express my sincere thanks to Dr. Ana Luisa Carvalho, academic tutor at DCV, for the continuous support and encouragement.

I place on record, my sense of gratitude to Fabrice Cordelières and Floriant Levet for developing some of the analytical scripts used throughout my internship.

I am also grateful to all the Choquet's laboratory members for the technical support, scientific discussions and friendship along this incredible year.

A special thanks to the Bordeaux Imaging Center, a service unit of the CNRS-INSERM and Bordeaux University, member of the national infrastructure France BioImaging for technical support in microscopy. A special thanks to the IINS molecular biology core facility for providing all the plasmids used in the current work. The IINS cell biology core facility is also here acknowledge.

Finally, I would like to thank my family and friends, who directly or indirectly, have supported me throughout this venture. A special thanks to Joana Ferreira for helping me "find my way back to Coimbra".

Table of contents

List of Abbreviations

AMPAR	α-amino-3-hydroxy-5-methyl-4-isoxazole propionic acid receptor
AP2	Clathrin adaptor protein
ATD	Amino terminal domain
BSA	Bovine serum albumin
CaMKII	Calcium/Calmodulin-dependent protein kinase II
cDNA	Complementary DNA
CGN	Cerebellar granule neurons
CKAP44	Cystine-knot AMPAR modulating protein 44 kD
CNIH	Cornichon homologs
Co-IP	Co-immunoprecipitation
CTD	C-terminal domain
DG	Dentate Gyrus
DHPG	Dihydroxyphenylglycine
DIV	*Days in vitro*
dSTORM	direct Stochastic Optical Reconstruction Microscopy
EGFP	Enhanced Green Fluorescent Protein
EPSC	Excitatory Postsynaptic Current
ER	Endoplasmatic Reticulum
FLIM	Fluorescence-lifetime imaging
FRET	Fluorescence Resonance Energy Transfer
HEPES	4-(2-hydroxyethyl)-1-piperazineethanesulfonic acid
iGLuR	Ionotropic glutamate receptors
IRES	Internal ribosome entry site
KAR	Kainate receptors
KD	*Knock-Down*
KO	*Knock-out*

LBD	Ligand binding domain
LTD	Long-term depression
LTP	Long-term potentiation
MAGUK	Membrane-associated guanylate kinase
mEPSC	Miniature excitatory postsynaptic currents
mGLUR	Metabotropic glutamate receptor
MSD	Mean Square Displacement
NMDAR	N-methyl-D-aspartate receptor
PBS	Phosphate buffered saline
PDZ	PSD95/Discs-large/ZO-1 homology domain
PFA	Paraformaldehyde
PKC	Protein Kinase C
PPR	Paired-pulse ratio
PSD	Postsynaptic density
RT	Room Temperature
shRNA	small hairpin RNA
SNARE	soluble N-ethylmaleimide-sensitive factor attachment protein receptors
TARP	Transmembrane AMPA receptor regulatory protein
uPAINT	Universal Point Accumulation Imaging in Nanoscale Topography

Abstract

α-amino-3-hydroxy-5-methyl-4-isoxazolepropionate (AMPA) subtype of glutamate receptor (AMPAR) mediate most of the fast excitatory synaptic transmission within the mammalian central nervous system. The number of AMPARs concentrated at the synapse strongly impacts the efficacy and properties of the synaptic transmission. This number can be dynamically regulated by a three-step mechanism, involving: (1) exo and endocytosis occurring at extrasynaptic sites; (2) lateral diffusion within the membrane plane and (3) receptor accumulation in synaptic nanodomains. AMPARs are formed of a core heterotrimeric structure of different subunits, surrounded by distinct auxiliary proteins that regulate both receptor trafficking and biophysical properties. Interactions with cytosolic scaffolding elements accumulated at the postsynaptic density (PSD) allow auxiliary proteins to regulate AMPAR surface mobility, determining the molecular organization of synaptic AMPARs. Unpublished data recently identified Shisa6 as a new *bona fide* AMPAR auxiliary protein. Being expressed throughout the hippocampus, Shisa6 directly interacts with AMPARs at the synapse and prevents receptor desensitization during prolonged presence of glutamate. Shisa6 also interacts with the scaffold PSD-95 through its PDZ ligand-binding motif, and potentially regulates AMPARs synaptic stabilization. The present study took advantage of different microscopy techniques to further explore the relationship between Shisa6 and AMPAR. Wide field microscopy suggested that Shisa6 is preferentially expressed in distal synaptic regions where it impacts spine morphology development. dSTORM showed that Shisa6 *KO* does not impact AMPAR organization at the nanoscale level in both proximal and distal dendritic regions. Moreover, this effect is not associated with changes in the number of AMPARs at the cell surface. Using uPAINT it was demonstrated that Shisa6 is able to regulate AMPAR surface mobility in distal dendritic regions. Interestingly, this effect appears to be dependent on interactions between Shisa6 PDZ ligand-binding motif and synaptic scaffolding elements. Moreover, this new AMPAR auxiliary protein is able to differentially regulate AMPAR surface mobility between proximal and distal dendritic regions.

Keywords: AMPAR; AMPAR auxiliary proteins; Shisa6; Super-resolution microscopy; Lateral diffusion; Nanoscale organization.

Resumo

Os recetores do glutamato do tipo AMPA são os principais responsáveis por mediar a transmissão rápida excitatória no sistema nervoso central dos mamíferos. O número de recetores AMPA na sinapse influência grandemente as propriedades e eficiência da transmissão sináptica. Este número pode ser dinamicamente regulado por um mecanismo dividido em três etapas: (1) exo- e endocitose em zonas extrasinápticas; (2) difusão lateral membranar e (3) acumulação dos recetores em nanodomínios. Os recetores AMPA são estruturas heterotriméricas compostas por diferentes subunidades, rodeadas por proteínas auxiliares distintas, que podem regular tanto o tráfego de recetores como as suas propriedades biofísicas. As interações com proteínas intracelulares localizadas nas densidades pós-sinápticas permitem a estas proteínas auxiliares regular a mobilidade dos recetores AMPA à superfície, e determinam a organização molecular dos recetores AMPA sinápticos. Resultados recentes (não publicados) identificaram a proteína Shisa6 como uma nova e importante proteína auxiliar dos recetores AMPA. Esta proteína, Shisa6, é expressa por todo o hipocampo, e interage diretamente com os recetores AMPA na sinapse, e evita a dessensibilização dos recetores durante a presença prologada de glutamato. A Shisa6 interage também com a proteína âncora PSD-95, através do seu domínio de ligação PDZ, esta interação parece regular a estabilização sináptica dos recetores AMPA. No presente estudo utilizou-se diferentes técnicas de microscopia para explorar em profundidade a relação entre a Shisa6 e os recetores AMPA. Utilizando microscopia de fluorescência detetámos que a proteína Shisa6 é expressa preferencialmente em regiões sinápticas distais, e é capaz de modular a morfologia das espículas dendríticas. Microscopia de super-resolução dSTORM permitiu-nos observar que no modelo animal que não expressa a proteína Shisa6 (Shisa6 *KO)* não existe uma alteração da nanorganização dos recetores AMPA, quer nas regiões dendríticas proximais ou distais. Este efeito não está relacionado com alterações nos números de recetores AMPA superficiais. Utilizando a técnica de super-resolução uPAINT, demonstrámos que a Shisa6 regula a mobilidade superficial dos recetores AMPA nas regiões dendríticas distais. Este efeito parece estar relacionado com a interação entre o domínio de ligação PDZ da Shisa6 e as proteínas âncora sinápticas. Observámos ainda que esta nova proteína auxiliar dos recetores AMPA regula de forma distinta a mobilidade dos recetores AMPA à superfície entre as zonas dendríticas proximais e distais.

Palavras-chave: recetores AMPA, proteínas auxiliares dos recetores AMPA, Shisa6, microscopia de super-resolução, difusão lateral, nano-organização.

General Introduction

General Introduction

Structure of an excitatory chemical synapse

Neurons are specialized cells of the nervous system. Each neuron is able to communicate with hundreds of others, shaping complex circuitries responsible to control both emotions and behaviors (Ho et al., 2011). Such communication occurs in highly specialized cellular contacts, called synapse. Synapses are formed by the axon terminal of the sending neuron and the dendrites of the receiving one. The axon terminal forms the presynaptic part of the synapse that is separated by a synaptic cleft from the dendritic part, the postsynapse. Neurotransmitter released into the synaptic cleft by the presynapse, binds to specific receptors accumulated in the postsynaptic membrane. In the case of the excitatory chemical synapse, the main neurotransmitter is glutamate (Meldrum, 2000). Binding of glutamate to defined ionotropic receptors leads to the opening of ion channel pore, with the concomitant influx of positively charged ions across the neuronal membrane. This triggers diverse downstream signaling events which generate a postsynaptic depolarization and engage different synaptic plasticity mechanisms.

The majority of the excitatory neurotransmission occurs in dendritic spines, defined as small protrusions emerging from the dendritic shaft (Sheng and Hoogenraad, 2007). Each spine consists of head connected to the dendrites by a thin spine neck. The cytoplasm of this postsynaptic structure has different components: (1) the PSD, a crowded accumulation of different synaptic proteins; (2) a rich meshwork of cytoskeletal elements (Lamprecht and LeDoux, 2004); (3) organelles from the exocytic pathway (Ehlers, 2013), and (4) different endosomal compartments (Park et al., 2006). The PSD is normally localized beneath the plasma membrane opposing the neurotransmitter release sites, forming a disk-like proteinaceous structure (fig.1). This specialization is composed of hundreds of different proteins, which include membrane receptors, cytoplasmatic scaffolding elements, signaling enzymes, and cytoskeletal proteins (Sheng and Kim, 2011). Scaffolding proteins are central building blocks of the PSD as they dynamically organize different synaptic proteins to ensure a proper synaptic function. Synaptic scaffolding proteins contain multiple PDZ domains and are usually members of the membrane-associated guanylate kinases (MAGUK)-family of proteins (Xu, 2011). PSD-95, a prototypal member of the MAGUKs, is one of the best characterized postsynaptic scaffolding proteins (Cho et al., 1992). Due to their PDZ domains, synaptic scaffolds are essential to ensure the fidelity of the neurotransmission by organizing postsynaptic receptors in front of presynaptic glutamate release sites. Moreover, these scaffolds are responsible for the organization of multiple signaling molecules, guaranteeing an efficient activation of downstream pathways upon glutamate binding.

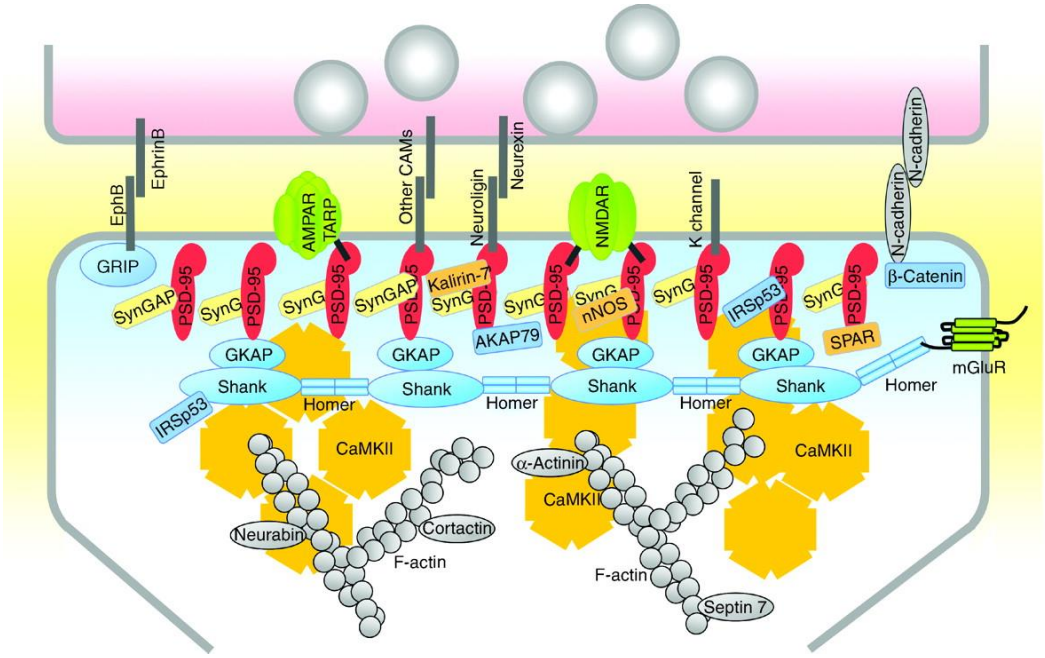

Figure 1 – Molecular organization of the postsynaptic density: schematic representation of the different family of proteins accumulated at the PSD: ionotropic channels and membrane receptors; intracellular scaffold (adaptor) elements; signaling molecules; components of the cytoskeleton; cell-adhesion molecules. Synaptic scaffolds are important to organize different synaptic proteins and due to protein-to-protein interactions are able to: (1) accumulate glutamate receptors in front of neurotransmitter release site; (2) link transmembrane proteins to different intracellular mediators, and (3) ensure an efficient activation of diverse downstream signaling pathways upon glutamate binding. Figure reproduced from (Sheng and Kim, 2011).

A remarkably property of dendritic spines is their morphological diversity. Classically, dendrites spines are divided into different gross morphologic categories: mushroom.-like spines presenting a large head and a narrow necks; thin spines formed by smaller heads and narrow necks; stubby spines with no constriction between the head and the attachment to the shaft; and a hair-like structure named fillopodium (Hering and Sheng, 2001; Nimchinsky et al., 2002). The structure of dendritic spines is highly dynamic, particularly during postnatal development, when massive number of spines are being made (Bhatt et al., 2009). At early developmental stages, dendrites are covered with filopodia that transiently protrude and retract from the dendritic shafts (Calabrese et al., 2006). This dendritic filopodia are accepted mediate activity-dependent synaptogenesis by facilitating the encounter between a developing axon and a targeted dendrite (Portera-Cailliau et al., 2003). As the development progresses, the numerous dendritic filopodia are gradually replaced by, or converted to, mushroom-like spines (Li and Sheng, 2003).

Glutamate Receptors

After release from the presynaptic terminal, glutamate acts through different metabotropic G-coupled protein receptors (mGluRs) and ionotropic receptors (iGluRs).

Glutamate signaling through mGluRs (mGluA1-A8) regulates diverse signaling pathways via a cascade that involves GTP-binding proteins (Niswender and Conn, 2010). mGluR activation

produces different intracellular messengers that ultimately modulates ion channel function at the plasma membrane. A good example of such modulation occurs during Dihydroxyphenylglycine (DHPG)-induced LTD (Xiao et al., 2001). Activation of mGLUR by DHPG may regulate several iGluRs, constributing to the depression of the synaptic response.

Ionotropic glutamate receptors are differential grouped in 4 classes based on agonist pharmacology. N-methyl-D-aspartate (NMDA) receptors (subunits GluN1, GluN2A-GluN2D, GluN3A and GluN3B) are ligand-gated channels characterized by high Ca^{2+} permeability, voltage-dependent blockage by extracellular Mg^{2+}, and glycine or D-serine as a co-agonist (Paoletti and Neyton, 2007). NMDAR are known as coincident detectors, because at hyperpolarized membrane potentials, extracellular Mg^{2+} blocks NMDAR ion channel; at depolarized membrane potentials, Mg^{2+} is released from its binding-site, allowing Na^{2+} and Ca^{2+} influx if glutamate and the co-agonist are present (Luscher and Malenka, 2012). The influx of Ca^{2+} through NMDAR activates different downstream signaling pathways, responsible to engage long-term changes in synaptic strength (Paoletti and Neyton, 2007; Luscher and Malenka, 2012). α-amino-3-hydroxy-5-methyl-4-isoxazolepropionate (AMPA) receptors (subunits GluA1-A4) are ligand-gated channels that show permeability to Na^{2+} and are critically involved in the fast synaptic transmission (Shepherd and Huganir, 2007; Traynelis et al., 2010). The dynamic regulation of AMPARs numbers at the synapse impacts the fidelity of synaptic transmission and regulates the expression of different plasticity events (Choquet and Triller, 2013; Huganir and Nicoll, 2013). Kainate (KA) receptors (subunits GluK1-K5) are ligand-gated ion channels permeable to Na^{2+} (Lerma and Marques, 2013). In addition to their role as ionotropic receptors, KA receptors also activate G-protein-coupled second messengers-mediated signaling cascades (Rodríguez-Moreno and Lerma, 1998). Due to such unusual properties, these receptors are responsible for (1) mediating postsynaptic depolarization at some synapses; (2) modulating neurotransmitter release, and (3) regulating the maturation of neuronal circuits along the development. δ receptors (subunits D1 and D2) are a less characterized family of glutamate receptors (Lomeli et al., 1993).

AMPA receptors

The AMPA subtype of glutamate receptors (AMPAR) mediates most of the fast excitatory synaptic transmission in the central nervous system (Shepherd and Huganir, 2007; Traynelis et al., 2010). Due to its fast kinetics, AMPARs are responsible for conveying "moment-to-moment" synaptic transmission and to mediate a primary postsynaptic depolarization in response to glutamate. AMPAR are ionotropic receptors formed by different tetrameric assemblies of four transmembrane subunits (GluA1-A4), which have different pharmacological and gating properties (Collingridge et al., 2009). Each AMPAR subunit is differentially expressed throughout the brain, presenting highly regional, developmental, and cell-specific regulation (Traynelis et al., 2010;

Schwenk et al., 2014). In the adult hippocampus, AMPARs are predominantly founded as GluA1/A2 and GluA2/A3 heteromers (Wenthold et al., 1996; Lu et al., 2009)

According to the recent crystallography study, AMPAR subunits are organized as a dimer of dimers (Sobolevsky et al., 2009). Each GluA subunit is a transmembrane protein composed by an extracellular amino terminal domain (ATD); a second extracellular domain forming the ligand binding domains (LBD); three hydrophobic transmembrane domains (M1, M3, and M4); a membrane reentrance loop (M2) forming the ion pore; two intracellular loops; and an intracellular C-terminal domain (CTD) with variable length (Traynelis et al., 2010) (fig.2). As a direct result, there are four ligand-binding sites in a tetrameric receptors, and a minimum of two of them needs to be occupied to activate the receptor (Robert and Howe, 2003).

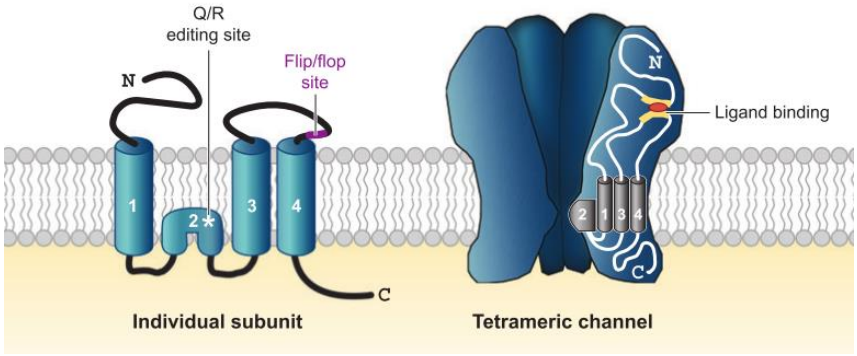

Figure 2 – Topology of an AMPAR subunit and its tetrameric organization: individual AMPAR subunits are composed by four transmembrane domains. All subunits are associated as dimers of dimers, in different combinations to form tetrameric ionotropic receptors. The biophysical properties of AMPARs are strictly dependent on the receptor subunit composition. At the hippocampus, AMPARs are present as GluA1/A2 and GluA2/A3 heterotrimeric combinations. Figure adapted from (Shepherd and Huganir, 2007).

AMPARs are subjected to different posttranscriptional and posttranslational modifications that directly impacts receptor functional properties (Santos et al., 2009). The LBD of all four GluA subunits occur in two alternative spliced isoforms – flip and flop (Sommer et al., 1990). Flip/Flop isoforms differ in their desensitization, resensitization, and deactivation kinetics, sensitivity to allosteric modulators, and cell-type specific distribution (Jiang et al., 2006; Shepherd and Huganir, 2007). Another peculiar property of AMPARs is the presence of a Q/R RNA editing site within the M2 pore loop of the GluA2 subunit (Shepherd and Huganir, 2007). Such editing leads to a change of a glutamine (CAG) for an arginine codon (CIG) and occurs in almost all GluA2 transcripts (Traynelis et al., 2010). GluA2-containing AMPARs are characterized by low conductance and impermeability to Ca^{2+} (Greger et al., 2007). Moreover, the presence of this subunit gives AMPAR a linear current-voltage relationship, allowing either influx and efflux of cations according to the cell membrane potential (Liu and Zukin, 2007). In contrast, GluA2- lacking AMPARs are permeable to Ca^{2+} and only allow cation influx across the cell membrane. Consequently, the presence of the GluA2 subunit has a tremendous impact on AMPAR biophysical properties.

An important determinant of AMPAR dynamic properties is its intracellular CTD. GluA2 and GluA4 have an additional alternative splicing site in the CTD resulting in long and short isoform (Huganir and Nicoll, 2013). As a consequence, GluA1 and 4 generally have longer CTD than GluA2 and 3. These long and short CTDs have a variety of different phosphorylation sites and protein interactions that critically regulate AMPAR trafficking and signaling (Anggono and Huganir, 2012). Normally, receptors composed of subunits with short CTD (GluA2/3) are constitutively trafficked in and out of the synapse, whereas receptor with long CTD (GuA1/A2) are added into the synapses in an activity-dependent manner (Santos et al., 2009).

AMPAR functional properties are critically dependent on receptor conformational state. Glutamate binding to AMPAR induces conformational changes in the LBD and to the opening of the ion channel pore (Armstrong and Gouaux, 2000). The extent of ion influx through the channel is limited by (1) glutamate dissociation from LBD, a mechanism defined as receptor deactivation (Traynelis et al., 2010) (2) transition to a non-conducting desensitized state (Colquhoun et al., 1992). AMPAR desensitization can occur to brief and prolonged exposure to glutamate, where glutamate remains bound to the receptors even if the channel closes. The recovery from the desensitization occurs at variable timescales and can regulate AMPAR signaling during fast synaptic transmission (Jones and Westbrook, 1996; Xu-Friedman and Regehr, 2004).

AMPA receptor dynamic nano-organization

AMPARs are not stable entities at the synapse. Rather, these receptors are continuously recycling between different intracellular compartments and the plasma membrane by constitutive and activity-dependent mechanisms (Nicoll and Bredt, 2003; Collingridge et al., 2004). Dendritic spines have a functional endocytic pathway composed by early endosomes, recycling endosomes, multivesicular bodies, and lysosomes (Ehlers, 2013). These organelles are essential to orchestrate the trafficking of AMPARs to and from the plasma membrane. Indeed, they are the primary subcellular compartments where AMPARs can be mobilized or restricted to the plasma membrane in response to neuronal activity (Ehlers, 2000; Park et al., 2006). AMPAR insertion in the plasma membrane is mediated by SNARE-dependent exocytosis and can occurs: (1) at extrasynaptic sites in the dendritic shaft (Yudowski et al., 2007; Makino and Malinow, 2009) or (2) in perisynaptic sites in the spines at syntaxin-4 microdomains (Lledo et al., 1998; Kennedy et al., 2010). On the other hand, the removal of AMPARs from the plasma membrane is a dynamin-dependent process involving clathrin-coated pits and the AP2 adaptor protein (Carroll et al., 1999; Lee et al., 2004). This endocytic process occurs laterally to the PSD due to dynamin-3/Shank/Homer interactions (Racz et al., 2004; Lu et al., 2007).

After being inserted in the plasma membrane, AMPARs becomes extremely mobile (Borgdorff and Choquet, 2002). This mobility is powered by lateral (Brownian) diffusion and allows AMPARs to exchange between extrasynaptic and synaptic sites. Brownian motion is powered by thermal molecular agitation, causing apparent random trajectories of AMPARs at the cell membrane

(Triller and Choquet, 2008). Interestingly, the mobility of AMPARs at the cell surface is extremely heterogeneous, alternating within seconds between mobile and immobile states (Borgdorff and Choquet, 2002). During basal conditions, almost half of the AMPAR population present in cell membrane are mobile and almost 90% if only extrasynaptic regions are considered (Tardin et al., 2003; Heine et al., 2008). Importantly, extrasynaptic AMPARs can readily enter the synapse, scan the PSD surface, and eventually exit if not properly accumulated (Tardin et al., 2003; Bats et al., 2007; Heine et al., 2008). This numbers implies that extrasynaptic AMPARs can act a mobile pool of receptors for synaptic recruitment. To ensure a reliable synaptic communication, AMPARs needs to be properly accumulated in front of presynaptic neurotransmitter release sites (Lisman and Raghavachari, 2006). Considering the diffusional properties of AMPARs, how can them be efficiently accumulated at the PSD? This local clustering of AMPARs is mainly mediated through interactions with PDZ-containing scaffolding elements belonging to the MAGUK family of proteins (Kim and Sheng, 2004). In agreement, the canonical PSD-95 is believed to be particularly important to regulate the number of synaptic AMPARs (Ehrlich and Malinow, 2004). Another critical components of this mechanism are the AMPAR auxiliary subunits (discussed below). The major consequence of this crowded environment is the stalking of AMPARs and a decrease of its diffusional rate, by a process known as diffusional trapping (Choquet and Triller, 2013). Thus, the dynamic interplay between trafficking mechanisms and lateral diffusion is crucial to efficiently regulate the number of AMPARs at the PSD, where receptors are accumulated in order to mediate synaptic transmission (fig.3A).

The development of super-resolution microscopy techniques turned possible to revisit some classical concepts of the glutamatergic transmission by determining the molecular organization of synaptic proteins with an unprecedented resolution (Fukata et al., 2013; MacGillavry et al., 2013; Nair et al., 2013). Recent work from our lab showed that AMPARs are not homogeneously distributed inside the synapse but are rather accumulated in clusters of <100 nm in size, containing around 20-25 receptors (Nair et al., 2013). The diffusional behavior of synaptic AMPARs is extremely heterogeneous, with receptors being immobilized inside these nanodomains and highly mobile in between them. Modulation of the organization and receptor content of AMPAR nanodomains strongly impacts the efficacy of the postsynaptic response, suggesting that synaptic transmission can be modulated by receptor nano-organization. This nanoscale organization is not restricted to AMPARs but is also observed for other synaptic proteins such as the postsynaptic density protein 95 (PSD-95) (Fukata et al., 2013; MacGillavry et al., 2013). The classical view of a continuum composed by mobile receptors outside the synapse and immobile elements inside the synapse is largely misleading. Indeed, the postsynaptic membrane needs to be considered as a highly compartmentalized environment where synaptic molecules are organized in nanodomains.

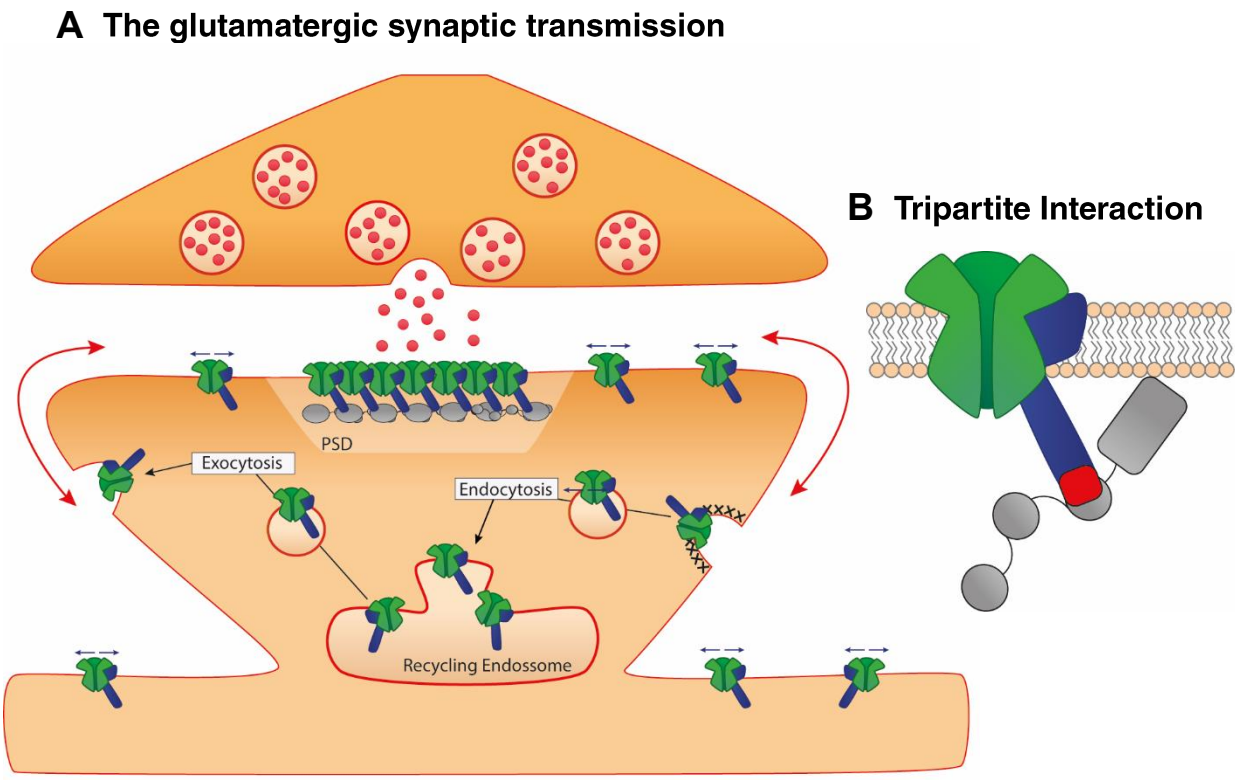

Figure 3 – The glutamatergic synaptic transmission. A) AMPARs undergo continuous recycling between different intracellular organelles from the secretory pathway (e.g., recycling endosomes) and the plasma membrane (black arrows). This constant turnover is powered by highly localized endo- and exocytic processes occurring laterally to the PSD. After reaching the cell membrane, AMPARs become mobile and due to lateral diffusion are able to exchange between extrasynaptic and synaptic regions (red arrows). The receptors are then stabilized and accumulated at the PSD, inside small clusters of <100 nm (nanodomains) in order to efficiently mediate synaptic transmission. **B)** A tripartite interaction regulates AMPAR nanoscale organization at the synapse: receptor per se (green), cytoplasmatic scaffolding elements (PSD-95: gray) and transmembrane auxiliary proteins (blue). The importance of AMPAR auxiliary proteins is critically discussed below.

AMPAR surface mobility is described to control synaptic transmission over timescale of a few tens of milliseconds (Heine et al., 2008; Constals et al., 2015). AMPAR are not all stabilized at the PSD and around half of the receptors are constantly diffusing in and out of the synapse (Borgdorff and Choquet, 2002; Tardin et al., 2003). Moreover, the distances travelled by mobile AMPARs within few milliseconds are theoretically enough to allow them to travel across large sections of the PSD (Choquet, 2010). This pool of mobile AMPARs is critical to exchange desensitized receptors by naïve ones upon glutamate release, maintaining the fidelity of the synaptic transmission during fast synaptic transmission (Heine et al., 2008; Constals et al., 2015). After a first stimulus, a large fraction of AMPARs is desensitized and lateral diffusion allows to exchange this inactive receptors for neighboring naïve ones, reducing the extent of paired-pulse depression. This hypothesizes is supported by different evidences: (1) immobilization of AMPARs through antibody-mediated cross-linking, potentiates paired-pulse depression (Heine et al., 2008); (2) accelerating AMPAR lateral diffusion by removing extracellular matrix enhanced recovery from paired pulse depression (Frischknecht et al., 2009) (3) AMPAR stabilization by PSD-95 increased

synaptic depression during high-frequency stimulation (Opazo et al., 2010). Thus, it is widely accepted that AMPAR lateral diffusion sustains higher frequencies of activity than the rate of AMPAR recovery from desensitization would normally allow (Choquet, 2010).

AMPAR surface mobility impacts the efficacy of the synaptic transmission for larger timescales (Choquet and Triller, 2013). The number of AMPARs at a given synapse is not fixed but greatly varies in function of synaptic activity (Lisman and Raghavachari, 2006). As above described, AMPAR trafficking is highly dynamic mechanism where AMPARs continuously shuttle between the plasma membrane and the different store pools to regulate their synaptic number. Remarkably, synaptic activity can dramatically change the balance of this dynamic mechanism to either promote or decrease the number of synaptic AMPARs (Shepherd and Huganir, 2007; Huganir and Nicoll, 2013). This activity-dependent changes of synaptic composition, known as synaptic plasticity, underlies mechanisms of learning and memory formation (Bliss and Collingridge, 1993). The best characterized forms of synaptic plasticity are long-term potentiation (LTP) and long-term depression (LTD) (Luscher and Malenka, 2012). LTP is defined by a long-lasting increases in the efficacy of synaptic response following a short high-frequency stimulation, whereas LTD is referred as a decreases in the synaptic strength, following a prolonged low frequency stimulation. Activation of NMDARs during postsynaptic depolarization leads to a rise of intracellular Ca^{2+} within the dendritic spine (Paoletti and Neyton, 2007). The magnitude of Ca^{2+} influx determines whether NMDAR activation results in LTP or LTD (Yang et al., 1999; Huganir and Nicoll, 2013). High levels of Ca^{2+} during LTP activates low-affinity kinases responsible to phosphorylate a broad range of proteins to selectively enhance synaptic transmission. On the other hand, a transient Ca^{2+} signal during LTD induction activates high-affinity phosphates (e.g., calcineurin) with the concomitant dephosphorylation of PSD proteins, reducing synaptic transmission (Yang et al., 1999; Luscher and Malenka, 2012). This differences of signaling pathways are responsible for a bidirectional regulation of synaptic AMPAR number, summarized by a three-step model (Opazo and Choquet, 2011). The increase of synaptic AMPARs during LTP is proposed to result from (1) increase of AMPAR exocytosis in extrasynaptic or perisynaptic sites; (2) lateral diffusion along the membrane plane and (3) increase of AMPAR clustering at the PSD. Furthermore, LTD is referred to consist in the reverse orders of events observed during LTP: (1) destabilization of synaptically anchored AMPARs; (2) removal to extra/perisynaptic sites via lateral diffusion and (3) increase of AMPAR endocytosis (Opazo and Choquet, 2011).

AMPAR auxiliary proteins

In native tissues, AMPAR are described as macromolecular complexes comprising an unprecedented complexity of different auxiliary proteins (Schwenk et al., 2012). The composition of the AMPAR proteome is highly dynamic, changing across different brain regions, during development or in response to neuronal activity (Schwenk et al., 2014). To be defined as a channel auxiliary subunit, a protein has to (1) be a non-pore-forming subunit; (2) direct and stable interact

with the pore-forming subunit; (3) modulate the channel and/or trafficking properties and (4) be required *in vivo* (Yan and Tomita, 2012). The *social-network* of AMPAR auxiliary proteins has been recently expanded, comprising a large number of subunits capable to differentially regulate AMPAR properties (fig.4).

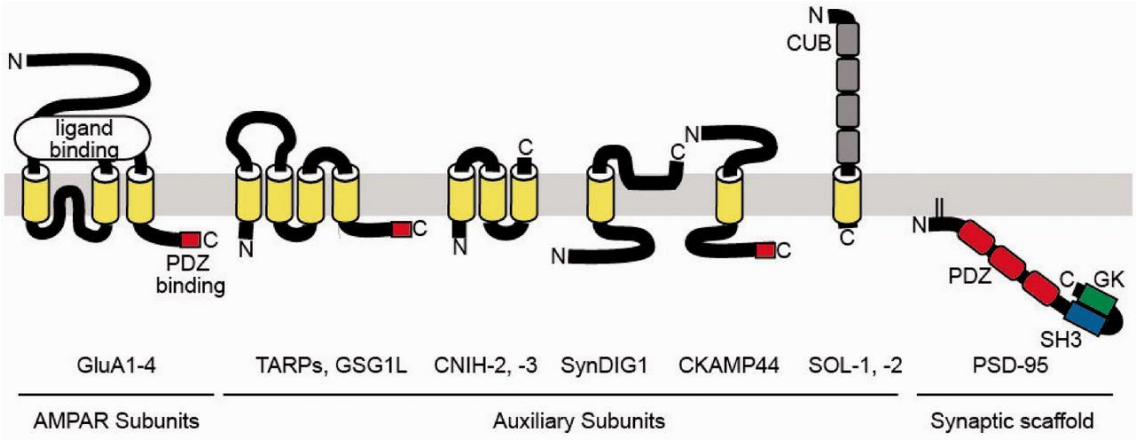

Figure 4 – Structural representation of an AMPAR subunit, its auxiliary subunit, and a scaffold protein: GluA1-4 AMPAR subunits; AMPAR auxiliary proteins: TARPs, GSG1L; CNIH-2,-3; SynDIG1; CKAMP44 (Shisa9, first identified member of the Shisa-like family of proteins); Sol-1, -2. PSD-95 scaffold protein. N, N-terminus; C, C-terminus; CUB, complement C1r/C1s, Uegf, Bmp1 domain; GK, Guanylate kinase domain; PDZ, post synaptic density protein (PSD-95)-Drosophila disc large tumor suppressor (Dlg1)-zonula occludens-1 protein; SH3, SRC homology 3 domain. Figure adapted from (Sumioka, 2013)

The first transmembrane auxiliary subunit to be described was stargazin (TARP γ-2) (Letts et al., 1998). Stargazin is a brain specific, low-molecular weight, tetraspanning membrane protein with homology to the voltage-gated Ca^{2+} channels subunit γ-1. Cerebellar granule neurons (CGN) lacking stargazin have a reduction on both AMPAR-mediated synaptic and extrasynaptic currents (Chen et al., 2000). This reduction is due to a decreased receptor number at the cell surface, demonstrating the critical role of stargazin in the trafficking and surface expression of AMPARs. Stargazin is a member of an extended family of Transmembrane AMPA receptor Regulatory Proteins, that includes the canonical type I TARPs (γ-2, γ-3, γ-4, and γ-8) and type II TARPs (γ-5 and γ-7) (Tomita et al., 2003; Kato et al., 2010). These homologous proteins have a widespread and overlapping expression through the brain that differs between different cell types and along the development. For example, TARP γ-8 is preferentially expressed in the hippocampus, and γ-8 *KO* selectively reduces extrasynaptic AMPAR function in this brain region (Rouach et al., 2005). Mass spectrometric analysis revealed that TARPs binds directly and non-preferably to all AMPAR subunits (Schwenk et al., 2012). Such interaction might occur earlier in AMPAR lifecycle, since stargazin is proposed to have an important role in AMPAR biosynthesis and ER export (Vandenberghe et al., 2005; Shanks et al., 2010). Moreover, TARPs are crucial regulators of AMPAR surface expression. Overexpression of a full-length form of stargazin, γ-3, γ-4, and γ-8 on CGN neurons lacking stargazin efficiently restores both synaptic and extrasynaptic AMPARs (Chen et al., 2000; Tomita et al., 2003). Another critical role for TARPs, and more particularly stargazin, is the anchoring of AMPARs at the PSD through binding to PDZ-domain containing

proteins like PSD-95 (Bats et al., 2007; Hafner et al., 2015). Disrupting the interaction between TARP PDZ domain and PSD-95 using divalent ligand strongly reduces AMPAR synaptic function (Sainlos et al., 2011). The regulatory role of TARPs on AMPAR synaptic expression is subjected to regulation by posttranslational modifications. The CTD of type I TARPs contains a conserved set of serine residues that are substrate for CaMKII and/or PKC phosphorylation (Tomita et al., 2005a). These serines are found within a highly basic region of the CTD able to interact with the acidic phosphate head groups of membrane phospholipids. Poly-serine phosphorylation is proposed to disrupt the interaction between TARP CTD and the plasma membrane, ensuring the synaptic localization of the AMPAR/TARP complex (Sumioka et al., 2010). Remarkably, TARP phosphorylation is bidirectional regulated by synaptic activity (Tomita et al., 2005a). TARPs phosphorylation and dephosphorylation are considered to occur during LTP and LTD, respectively. In agreement, synaptic trapping of pre-existing surface receptors through CaMKII-induced phosphorylation of stargazin is proposed to be an early even during synaptic potentiation (Opazo et al., 2010). Phosphorylation of stargazin was also elegantly shown to be involved in synaptic scaling mechanisms, a form of homeostatic plasticity translated by a proportional adjustment of AMPAR content to long-term neuronal activity alterations (Louros et al., 2014). Besides their role in trafficking, TARPs are also able to modulate AMPAR gating properties and pharmacology. It is described that stargazin slows the rate of desensitization and enhances the amplitude of steady-state currents of endogenous AMPARs (Priel et al., 2005). The co-expression of AMPARs and stargazin slows the rate of deactivation and increases the recovery from desensitization (Tomita et al., 2005b; Turetsky et al., 2005). The presence of stargazin potentiates the affinity of AMPARs to glutamate (Tomita et al., 2005b). A complete review regarding such modulation can be found elsewhere (Milstein and Nicoll, 2008; Jackson and Nicoll, 2011).

An additional component of the AMPAR macromolecular complex, cornichon-like proteins (CNIH), was identified by a systematic proteomic assay (Schwenk et al., 2009). This family includes two cornichon homologs (CNIH2 and CINH3) and forms a tripartite interaction with TARP γ-8 and AMPARs at the hippocampus (Kato et al., 2010). The expression of CNIH2/3 is significantly reduced in the hippocampus of TARP γ-8 *KO*, suggesting that this auxiliary protein stabilizes the CNIH/AMPAR complex in this brain region. CINH were initially reported to increase the surface expression, slow down desensitization and deactivation kinetics of AMPARs in heterologous cells (Schwenk et al., 2009). CNIH2/3 *KO* mice hippocampal neurons showed reduced AMPA-evoked currents and accelerated decay kinetics of AMPAR-EPSCs (Herring et al., 2013). In agreement with a cooperative effect between TARP γ-8 and CNIH2/3, CNIH2 slows the decay kinetics of TARP γ-8/AMPARs but not of TARP γ-2/AMPARs at the hippocampus (Kato et al., 2010; Herring et al., 2013). Besides regulating receptor trafficking and gating properties, CNIHs might impact AMPAR maturation in the ER. CNIHs share homology with Erv14p (yeast homolog) and Cornichon (drosophila homolog), a group of proteins that have an important role on the ER forward trafficking

to the Golgi apparatus (Jackson and Nicoll, 2011). CNIH2 serve as a cargo exporter protein from the ER, cycling between this structure and the Golgi apparatus (Harmel et al., 2012). The interaction between GluA subunits and CNIH2 is responsible for breaking this conserved role and the recruitment of the complex AMPA/CNIH2 to the cell surface. Moreover, this mechanism appears to be essential to mediate a homeostatic regulation of the neuronal excitability in *C. elegans* (Brockie et al., 2013). Indeed, Cni-1 (cornichon homolog) is responsible for limiting the AMPAR export from the ER and modifying receptor function to optimize neuronal excitability. However, it remains to be explored if CINHs play a similar role in AMPAR maturation in the CNS.

Shisa9 (formally denoted CKAMP44) was identified by immunopurification of native GluA1 AMPAR receptor complexes from forebrains (von Engelhardt et al., 2010). Shisa9 is a type I transmembrane proteins that contains an extracellular cysteine-rich motif, a single-span transmembrane region, and a type-II PDZ ligand-motif (EVTV). This auxiliary subunit is widely expressed throughout the brain with concentrated expression in DG granule cells. Shisa9 interacts with all GluA subunits and, in contrast to TARPs and CNIHs, prolongs deactivation, accelerates desensitization and slows the recovery from desensitization. As a consequence of its unusual properties, Shisa9 *KO* enhances the paired-pulse ratio (PPR) in DG granule neurons. By regulating AMPARs kinetics and channel properties, Shisa9 can profoundly impact synaptic short-term plasticity. Moreover, Shisa9 and TARP γ-8 might bind simultaneous to the same AMPAR complex in the DG granule cells (Khodosevich et al., 2014). Shisa9 and TARP γ-8 modulate some AMPAR properties in a similar fashion. Both proteins increases the time constant of deactivation and promoted receptor surface expression. Additionally, Shisa9 and TARP γ-8 impacts DG cell morphology and spinogenesis indirectly via the increase in the numbers of AMPARs on the cell surface (Khodosevich et al., 2014). However, there are particular regulatory functions that differ between these two AMPAR auxiliary subunits. Indeed, Shisa9 and TARP γ-8 show a different effects in short-term plasticity, which is due to the opposite influence on AMPAR desensitization. Remarkably, only TARP γ-8 is necessary for the activity-dependent control of synaptic receptor number during LTP. In agreement with a differential role between both proteins, no change in LTP was observed in Shisa9 *KO* DG granule cells (Khodosevich et al., 2014). Interestingly, Shisa9 is able to regulate the number of synaptic AMPARs during basal transmission, due to interactions with the PDZ domain-containing protein PSD-95. This interaction is dependent on Shisa9 putative PDZ ligand-motif, since no differences on mESPC amplitudes are seen when overexpressing a Shisa9 mutant lacking the EVTV domain (Khodosevich et al., 2014).

SynDIG1 is a type II transmembrane protein able to regulate AMPAR synaptic function and targeting (Kalashnikova et al., 2010). SynDIG1 colocalizes with AMPARs at synapses and extrasynaptic sites and regulates AMPAR content in developing synapses. SynDIG1 *KD* in dissociated hippocampal neurons lead to a reduction in AMPAR content, corroborating the role of this protein in AMPAR trafficking.

Sol-1 and -2 are type I transmembrane proteins containing four extracellular CUB-domains (Walker et al., 2006; Wang et al., 2012). In *C. elegans* both Sol-1 and -2 regulate the GLR1 (GluA homolog) desensitization and recovery from desensitization. Besides this modulatory role, both proteins appear to regulate AMPAR trafficking.

The claudin homolog GSG1L was recently characterized as an AMPAR auxiliary subunit (Shanks et al., 2012). Besides the structural homology with TARPs, the effect of their modulation of AMPAR properties is quite divergent. Indeed, the effect of GSG1L appears similar to Shisa9, by slowing down the recovery from desensitization. GSG1L might contribute to AMPAR trafficking, as revealed by the increase of receptor surface expression on HEK cells.

The development of different super-resolution microscopy techniques allowed to revisit some classical concepts of synaptic biology. Synapses are now considered highly dynamic entities in which all synaptic molecules act in concern to efficiently regulate synaptic communication (Choquet and Triller, 2013). In agreement, the dynamic molecular organization of AMPARs is reported to strongly impact the properties of the postsynaptic response (Nair et al., 2013). Remarkably, this fine organization is not restricted to AMPARs, but is also found in other synaptic molecules (e.g., PSD-95) (Fukata et al., 2013; MacGillavry et al., 2013). Since AMPARs do not directly interact with synaptic scaffolding elements, auxiliary subunits might have a preponderant role in AMPAR nanoscale organization (Bats et al., 2007) (fig.3B). Work from our lab has recently addressed the importance of this tripartite interaction (Constals et al., 2015). Glutamate application increases mobility of synaptic AMPARs. This effect is due to receptor desensitization and requires a decrease on AMPAR/stargazin interaction. Indeed, desensitized binds less stargazin and, by consequence, are less stabilized inside synaptic nanodomains. The increased mobility of desensitized AMPARs, efficiently renews the pool of receptors inside nanodomains, allowing a faster recovery from desensitization-mediated synaptic depression (Constals et al., 2015). Thus, AMPAR auxiliary subunits orchestrates the exchange of AMPARs between nanodomains, confirming the nanoscale importance of these proteins.

Shisa6: a new AMPAR auxiliary protein

Unpublished data recently characterized Shisa6 as a new *bona fide* AMPAR auxiliary protein (fig.5) (Klaassen et al., *in revision)*. Shisa6 belongs to the Shisa-like family of proteins and contains an extracellular cysteine-rich motif, a single-span transmembrane region, and a type-II PDZ ligand-motif (EVTV) at its intracellular C-terminal domain (Pei and Grishin, 2012). The cysteine-rich motif can form a cysteine-knot structure that, as described for Shisa9, might be a prerequisite for AMPAR biophysical modulation (Khodosevich et al., 2014).

Being expressed throughout the hippocampus, preliminary results showed that Shisa6 binds directly and non-preferably to AMPARs subunits GluA1-A3 at the synapse. The interactions between Shisa9 and AMPARs occurs intracellularly, involving a 20 amino acids stretch downstream to the transmembrane domains of Shisa9. However, such relationship on Shisa6 remains to be determined.

Shisa6 also interacts with PSD-95 through its PDZ ligand-binding motif, being a potential candidate to regulate AMPARs synaptic localization.

Shisa6 is responsible for keeping AMPARs in an activated state during prolonged presence of glutamate, preventing full desensitization and synaptic depression during high frequency stimulation. Indeed, Shisa6 decreases receptor desensitization and increases steady-state currents, an effect that is opposite to the one reported for Shisa9 (von Engelhardt et al., 2010). While Shisa9 slows down the recovery from desensitization, Shisa6 does not change it. Both Shisa9 and Shisa6 prolong deactivation kinetics. Besides this recent characterization, the precise role of Shisa6 in AMPARs surface mobility and molecular organization during basal transmission remains to be determined.

Aim and study outline

The main aim of the present study was to determine the role of Shisa6 in AMPAR surface mobility and nano-organization. A combination of different microscopy techniques was applied to further describe the relationship between Shisa6 and AMPAR in hippocampal neurons. A complete characterization was performed to determine if Shisa6 differentially regulates AMPAR mobility between proximal and distal dendrites. Moreover, a distance-dependent role for Shisa6 was evaluated.

Wide field microscopy was used to characterize the effect of Shisa6 acute manipulation in rat hippocampal neurons. The subcellular expression of this new auxiliary subunit was determined by quantification of the EGFP::Shisa6 surface labelling. A systematic analysis was undergone to evaluate if Shisa6 has a distance-dependent synaptic expression gradient. Additionally, it was also determine if this protein impacts spine morphology development. For this, endogenous Shisa6 levels were acutely manipulated along the development and spine morphology estimated from wide field images.

A combination of different super-resolution microscopy was applied to understand if Shisa6 differentially regulates AMPAR between proximal and distal dendrites. dSTORM was used to assess the role of Shisa6 in AMPAR nano-organization. This was performed by estimating the number of AMPARs inside nanodomains from Shisa6 *KO* mice hippocampal neurons. dSTORM was also used to evaluate if Shisa6 promotes AMPAR surface expression. From the obtained super-resolved images it was possible to quantify if Shisa6 *KO* changes the number of AMPARs at the cell surface. The effect of Shisa6 in AMPAR surface mobility was clarified using uPAINT microscopy. This technique was applied to study how Shisa6 *KO* affects AMPAR lateral diffusion in mice hippocampal neurons. AMPARs were also tracked by uPAINT on rat hippocampal cultures when endogenous Shisa6 levels were acutely manipulated. A mutant Shisa6 lacking the putative PDZ binding-motif was used to determine the dependence of the interaction with intracellular scaffolding elements. Finally, the surface mobility of overexpressed EGFP-Shisa6 in both proximal and distal dendrites was characterized.

A **Shisa6 is a transmembrane protein**

B **Shisa6 is highly expressed at the hippocampus and interacts with AMPARs**

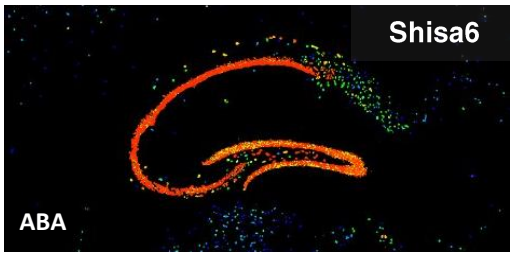

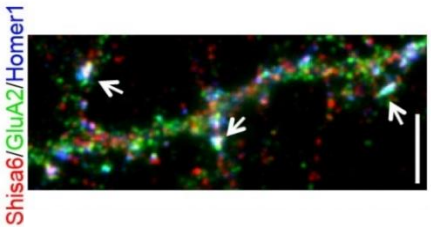

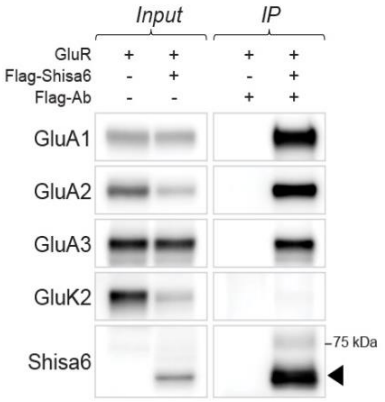

C **Shisa6 interacts with PSD-95 in a PDZ domain-dependent manner**

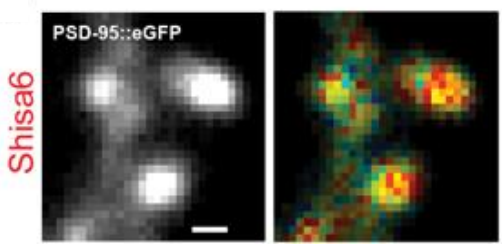

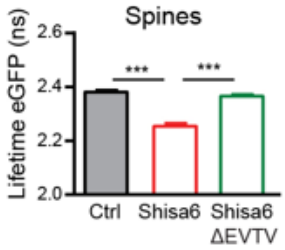

D **Shisa6 prevents AMPAR desensitization**

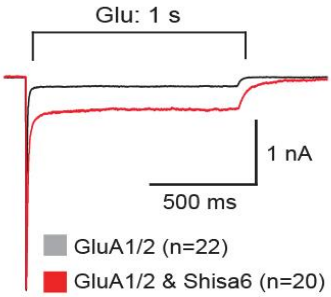

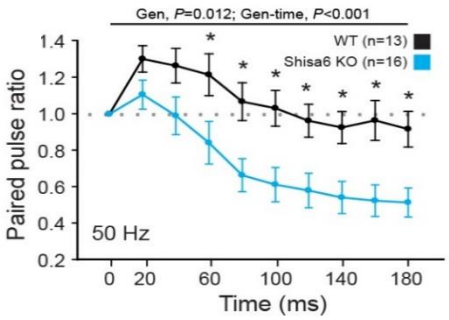

Figure 5 – Shisa6 is a new AMPAR auxiliary protein. Recent work from our lab characterized Shisa6 as a new *bona fide* AMPAR auxiliary protein (Klaassen et al., in revision). **A)** Shisa6 is a non-pore forming subunit containing an extracellular cysteine-rich motif, a single-span transmembrane region, and a type-II PDZ ligand-motif (EVTV) at its intracellular C-terminal domain. **B)** Shisa6 is expressed throughout the hippocampus (*left panel up*) and binds to AMPARs at synapse (*left panel bottom*: immunofluorescence of GluA2 and Shisa; *right panel*: Flag-Shisa6 binds directly to homomeric GluA1, A2, A3 (Co-IP). ABA: Allen Brain Atlas (www.brain-map.org). **C)** Fluorescence lifetime imaging (FLIM) suggests that Shisa6 is also able to interact with PSD-95 (decrease of EGFP lifetime, red plot). This interaction is lost when Shisa6 is lacking the EVTV domain (Shisa6 ΔEVTV, green plot). **D)** Shisa6 is responsible to prevent receptor desensitization and synaptic depression during high frequency stimulation. *Left panel:* Whole-cell recording from HEK293 cells expressing AMPARs without (grey) or with Shisa6 (red). *Right panel:* Paired-pulse ratios of electrically-evoked excitatory postsynaptic currents from hippocampal CA1 pyramidal cells of Shisa6 *KO* and *wild-type* littermates.

Material and methods

Material and Methods

Constructs. Flag::Shisa6-IRES-EGFP (clone Flag::Shisa6) was provided by G. Smit lab. This plasmid contains a FLAG-tag sequence between the codon 44 (ATC, Isoleucine) and the codon 37 (CAC, Histidine) of Shisa6 cDNA (reference: XM_006533619.2), and soluble EFGP under regulation of an IRES sequence. Due to the presence of the IRES sequence, the expression of the soluble EGFP act as a reporter for Flag-Shisa6 expression. EGFP::Shisa6 (clone EGFP::Shisa6) was constructed in the lab. This plasmid contains an EGFP-tag located in the same Shisa6 site than the Flag epitope of Flag::Shisa6. EGFP::Shisa6 EVTV (clone EGFP::Shisa6EVTV) contains the same EGFP-tag than EGFP::Shisa6 but lacks the putative PDZ domain-binding motif (EVTV) present in the last 4 aminoacids of its intracellular C-terminus. Shisa6 shRNA (clone shRNA::Shisa6) was provided by G. Smit lab. GFP::Shisa6 rescue (clone EGFP::Shisa6-Rescue) was constructed in the lab. This constructs contains the same cDNA sequence than shRNA::Shisa6 and a mutated variant of EGFP::Shisa6 resistant to the shRNA. Soluble EGFP (clone EGFP) was constructed in the lab.

Cell culture and transfection. Preparation of hippocampal neuronal cultures were performed as described in (Nair et al., 2013). Hippocampal neurons from 18 gestational-days-old rat embryos of either sex were cultured on glass coverslips following the banker protocol (Kaech and Banker, 2006). Briefly, dissociated neurons were plated on poly-L-lysine coated glass coverslips and co-cultured over an astroglial feeder layer in Neurobasal medium supplemented with SM1. Primary rat hippocampal neurons were transfected using Effectene at 7–9 *days in vitro* (DIV) with 1) Flag::Shisa6, shRNA::Shisa6, and EGFP::Shisa6EVTV in combination (except for Flag::Shisa6) with EGFP and (2) EGFP::Shisa6, and EGFP::Shisa6EVTV for uPAINT experiments on endogenous GluA2-containing AMPARs and overexpressed EGFP::Shisa6, respectively. uPAINT experiments on rat hippocampal neurons were performed at 13-16 DIV. Rat hippocampal cultures used in wide field microscopy experiments were transfected as previously described with shRNA::Shisa6, EGFP::Shisa6, and Shisa6::Rescue in combination with EGFP. Wide field microscopy experiments were sequentially performed at 10-14 DIV, and 21 DIV. Mice hippocampal cultures were derived from both *wild type* (C57BL6J) and Shisa6 *knockout* (*KO*) mice strains obtained as in unpublished data from our lab (Klaassen et al., *in revision).* Primary hippocampal neurons were derived from postnatal mice P0 or P1 of either sex and cultured on glass coverslips as previously described. uPAINT and dSTORM experiments on mice hippocampal neurons were performed at 13-16 DIV.

Immunocytochemistry. Rat hippocampal cultures used in wide field microscopy experiments were live stained with mouse-anti-GluA2 antibody (gift from E. Gouaux, Portland, OR) and rabbit-anti-EGFP antibody (A6455, Life Technologies, Carlsbad, CA) for 10 minutes at 37ºC. Mice hippocampal cultures used in dSTORM experiments were incubated with the same antibody to label endogenous GluA2-containing AMPARs. All samples were then fixed using 4%

paraformaldehyde (PFA) and 4% sucrose in phosphate-buffered saline (PBS). After three washes in PBS, they were incubated with NH_4Cl 50 mM (Sigma-Aldrich, St. Louis, MO) for 15 minutes to quench aldehyde reactive groups. Rat hippocampal neurons transfected with EGFP and shRNA::Shisa6 were additionally permeabilized with 0.2% Triton X-100 (Sigma-Aldrich, St. Louis, MO) in PBS during 5 min. After three washes in PBS, EGFP and shRNA::Shisa6 samples were incubated with PBS containing 1% Bovine Serum Albumine (BSA) (Sigma-Aldrich, St. Louis, MO) for 45 minutes followed by mouse-anti-PSD95 antibody (MAI-046, Thermo Scienfitic, Waltham, MA) incubation during 1 h at room temperature (RT). After three washes in PBS, all samples were then incubated with PBS containing 1% BSA for 45 minutes. The primary antibodies were revealed by incubating with a combination of IgG specific Alexa 647 coupled anti-mouse (A21245; A21242, Invitrogen, Paisley, UK), IgG specific Alexa 568 coupled anti-mouse (A21124; Invitrogen, Pasiley, UK), and Alexa 568 coupled anti-rabbit (A11036, Invitrogen, Pasiley, UK) secondary antibodies for 30 min at RT. Coverslips were finally rinsed three times in PBS-BSA 1% and three times with PBS before being fixed again, using previously described protocol.

Wide field fluorescence microscopy. Images of double-stained rat neurons were obtained by a Leica DM5000 (Leica Microsystems, Wetzlar, Germany) equipped with a HCX PL APO 100X oil NA 1.40 objective. A LED SOLA light (Lumencor, Beaverton, USA) was used for fluorescence excitation and the recordings were done using a resolutive camera CoolSnap HQ2 (Photometrics, Tucson, USA). Regions of interest (ROI) of both proximal and distal dendritic sites were systematically defined as indicated in (Shipman et al., 2013) by wavelet image segmentation of the EGFP signal. Proximal ROI were selected until the first dendritic branch (50 – 120 μm from the cell body) and distal ROI from the last dendritic segments (220 – 290 μm from the cell body) of the transfected neurons. Mosaics of the selected ROI were recorded using a motorized stage Scan (Märzhäuser, Wetzlar, Germany) in combination with a galvanometric stage (Leica Microsystems, Wetzlar, Germany) for Z stack control. The final images were reconstructed from the acquired mosaics as described in (Preibisch et al., 2009).

Spine morphology and fluorescence intensity analysis. Spine morphology was estimated from wide field images of endogenous GluA2-containing AMPARs in combination with overexpressed EGFP::Shisa6 (overexpression and rescue experiments) or endogenous PSD-95 (Shisa6 *KD* and control littermates), using a custom-made analysis module operating inside ImageJ software. For each ROI, dendritic spines were identified and isolated by wavelet segmentation of the EGFP signal. The segmented object was then computed to extract the aspect ratio, a simple morphology estimation determined by the ratio between the major and the minor axis of the identified spines. The represented aspect ratio corresponds to the median value of the all spines analysed. Spine segmentation was additionally used to extract fluorescence intensity of the Alexa 568 (GFP::Shisa6) signals within the same delimited region.

Single molecule localization principle. Due to the light diffraction it is virtually impossible to resolve objects within a precision of 200–350 nm using traditional fluorescence microscopy. Considering the average size of the synapse (~1 μm) and the high density number of different synaptic proteins, these techniques are largely unable to resolve the organization and dynamics of individual molecules. A detailed picture of the synapse demands microscopy techniques that circumvent the resolution limit, allowing the tracking and determination of multimolecular organization of synaptic proteins with nanometric sensibility. These requirements were fulfilled by the development of different super-resolution microscopy techniques. In single particle based super-resolution a subdifraction limited resolution is ensured by a deconvolution in a time-dependent manner of the fluorescence emission (fig.6). By recording a sparse population of fluorescent molecules per image, each single molecule is detected as a typical airy function possible to be fitted to a 2D Gaussian distribution. If the intensity of the signal is sufficiently high, the position of the centroid of this fit determines a sub-pixel localization of the molecule that overwhelms the diffraction limit. Super-resolved images containing all the molecular coordinates are then created by combining the accumulation of localizations along the experiment. The final super-resolved image can be reconstructed at a 20 nm pixel size, resulting in an increase of effective resolution by a factor of 8.

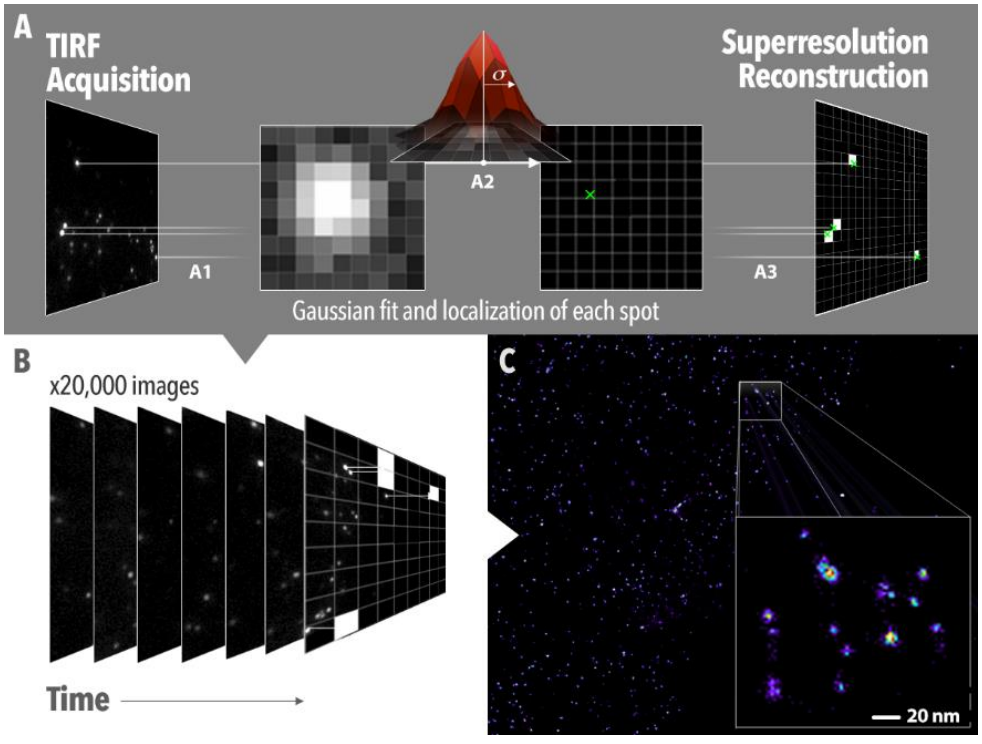

Figure 6 – Single particle localization microscopy allows to surpassing the diffraction limit. A) In single particle based super-resolution microscopy, a sparse and stochastic population of single molecules is imaged along the time (frame by frame). Due to the light diffraction, the fluorescence signal of each single molecule spreads in the space as a typical airy function possible to be fitted to a 2D Gaussian distribution. **B)** This fitting turns possible determining the position of the single molecule in a sub-pixel localization independently of the resolution limit. By using specific algorithms, super-resolved reconstructed images are then reconstructed by combining the accumulation of localization from different diffraction-limited acquired along the experiment. **C)** The final super-resolved image can be reconstructed at a 20 nm pixel size, resulting in an increase of effective resolution by a factor of 8. Figure provided by Corey Butler (not published).

Direct Stochastic Optical Reconstruction Microscopy (dSTORM). dSTORM is a single particle based super-resolution microscopy technique (fig.7A) (van de Linde et al., 2011). As described by van der Linde and colleagues, dSTORM explores the use of photoswitchable fluorescent probes and traditional immunostaining methods to render fluorescence of the sample. The density of labelling is rendered sparse enough for single molecule localization by switching the majority of the fluorophores to a dark metastable state prior to imaging. Due its metastability, fluorophores can stochastically return to the fluorescence cycle. This principle allows the record of a sparse population of fluorophores, creating conditions for single particle detection. Here we applied dSTORM to study the role of Shisa6 in AMPAR nano-organization due to the possibility of labelling endogenous GluA2-containing AMPARs and to its high localization accuracy. The stained coverslips were imaged within the following week at RT in a closed chamber (Ludin Chamber, Life Imaging Services) mounted on an Leica SR GSD 3D (Leica Microsystems, Wetzlar, Germany) as described elsewhere (Constals et al., 2015). Imaging was performed in an extracellular solution containing reducing agents and enzymatic oxygen scavengers. Proximal and distal regions were selected as previously indicated. Ensemble fluorescence of Alexa 647 were first converted in a metastable dark state using a 500 mW 642 nm (Coherent) at 60% of its intensity, respectively. Once the ensemble fluorescence was converted into a sparsely population of single emitters per frame, the laser power was reduced to 30 % of its total intensity and imaged continuously at 50 frames per second for 20,000 frames. The laser powers were adjusted to keep an optimal level of stochastically activated molecules during all the acquisition. Both the ensemble and single molecule fluorescence was collected by the combination of a dichroic and emission filter (D101-R561 and F39-617, respectively, Chroma, USA) and quad-band dichroic filter (Di01-R405/488/561/635, Semrock, USA). The fluorescence was collected using a sensitive iXon3 EMCCD camera (ANDOR, Belfast, UK). Single molecule localization and reconstruction was performed using LEICA Las Af software (Leica Microsystems, Wetzlar, Germany). Multicolor fluorescent microbead (Tetraspeck, Invitrogen Pasiley, UK) were used as fiduciary markers to register long-term acquisitions and correct for lateral drifts and chromatic shifts.

Universal Point Accumulation in Nanoscale Topography (uPAINT). uPAINT is a single particle based super-resolution microscopy technique that allows the study of the dynamic properties of endogenous transmembrane proteins on living cells (fig.7B) (Giannone et al., 2010). This technique is based on the continuous and stochastic labelling of transmembrane proteins at the cell membrane with fluorescent ligands in solution to provide high-density localizations of isolated single-molecule events. By (1) extracting the coordinates of all the single-molecule events in each frame and (2) connecting all the localized molecules through the time using appropriate algorithms, it is possible to extract molecular trajectories and dynamics (Sibarita, 2014). Trajectories analysis allows discerning between different modes of motions of the tracked molecules, giving detailed information of molecular organization and cellular processes at the single cell level. Here we applied uPAINT to determine the impact of Shisa6 in AMPAR lateral diffusion because (1) explores smaller and brighter

probes to obtain molecular trajectories; (2) achieve results at nanometric accuracy and millisecond temporal resolution; (3) obtain a high density number of molecular trajectories and (4) have access to large statistics (Cognet et al., 2014; Sibarita, 2014). Coverslips containing rat or mice hippocampal neurons (density ~20,000 cells/cm^2) were mounted on a Ludin chamber (Ludin chamber, Life Imaging Services, Switzerland) filled with 1 mL of HEPES-based solution Tyrode's at 37º C as indicated in (Constals et al., 2015). The osmolarity was adjusted before each experiment with NaCl and Neurobasal medium supplemented with B27 to match the culture medium. To track endogenous GluA2-containing AMPARs, the anti-GluA2 antibody labelled with ATTO 647N-NHS-ester (Atto-tec, Siegen, Germany) was used. Overexpressed EGFP::Shisa6 where tracked using an anti-EGFP nanobody labelled with ATTO 647N-NHS-ester (Atto-tec, Siegen, Germany), as described previously (Giannone et al., 2010). Proximal and distal regions were selected as previously indicated. The chamber was mounted on an inverted microscope (IX71; Olympus America, Melville, NY) equipped with a high 100X objective (1.49 NA) and a charge-coupled device camera (Cascade 128; Roper Scientific, Princeton Instruments, Trenton, NJ). The stochastic labelling of the targeted protein by dye couples antibodies allowed the recording of thousands of trajectories lasting longer than 1 s. A HeNe laser was used in oblique illumination mode for excitation of both dyes. Recordings were made at 20 Hz using Metamorph software (Molecular Devices, USA) in streaming mode. Multicolor fluorescent microbeads (Tetraspeck, Invitrogen) were used to record long-term acquisitions and correct for lateral drifts.

Single molecule localization and tracking. A typical uPAINT experiment acquired with the aforementioned protocol produced a set of 4,000 to 8,000 images that are analysed to extract molecule localization and dynamics. All the single molecule fluorescent spots were localized in each frame and tracked over the time as previously described (Nair et al., 2013). The software package used to derive quantitative data on protein localization is custom written as a plug-in running within the MetaMorph software environment. For the trajectory analysis, transfected neurons were identified by wavelet image segmentation of the soluble EGFP signal. The corresponding binary mask was defined by threshold and used to sort single particle data analysis to specific synaptic and dendritic regions. MSD curves was calculated for reconnected trajectories of at least 10 frames. Diffusion coefficients were calculated by a linear fit of the first 4 points of the MSD plots versus time.

Super-resolution cluster analysis. AMPAR nanodomains were identified from super-resolved images using custom software as a plug-in running inside MetaMorph. Nanodomains, clustered areas where the signal-to-noise ratio was higher, were identified by wavelet segmentation. Nanodomain number and dimensions were then computed by 2D anisotropic Gaussian fitting, from which the principal and the auxiliary axes were extracted as $2.3\sigma_{\mathrm{long}}$ and $2.3\sigma_{\mathrm{short}}$ respectively. All synaptic analysis were done in mushroom shaped spines identified by wide field fluorescence images of the GluA2 surface labelling.

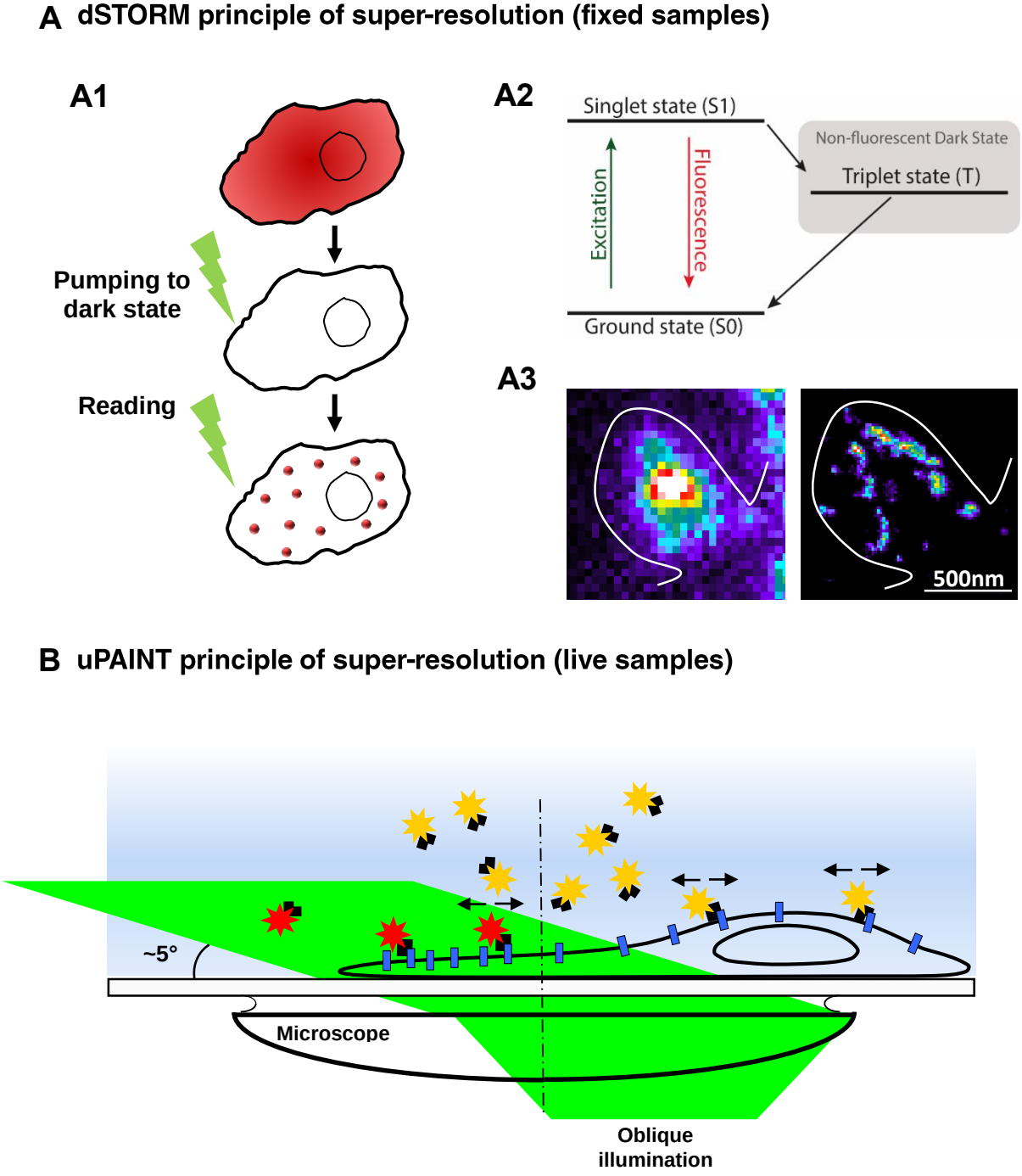

Figure 7 – Theoretical principal of uPAINT and dSTORM super-resolution microscopy. A1) dSTORM is based on the recording of a sparse and stochastic population of single molecules along the time. All fluorophores present in the fixed sample are converted to a dark metastable state prior to imaging. A stochastic population is reactivated (fluorescent cycle) creating conditions for single particle detection. **A2)** Jablonski diagram of a fluorophore in dSTORM conditions. The triplet state is ensured by a combination of thiols solution and oxygen scavengers. **A3)** Image of synaptic GluA2-containing AMPARs recorded by dSTORM (*left panel*: low resolution image; *right panel:* super-resolved image of the same region). **(B)** Schematic representation of the uPAINT microscopy: continuous and stochastic labeling of membrane proteins with fluorescent ligands and imaging the sample in oblique illumination. A low concentration of fluorophores is added to the recording chamber. The oblique illumination ensures that only fluorophores bond to transmembrane proteins are excited. Since the fluorescent ligands free in solution are not excited, a constant rate of membrane molecules is labeled during the imaging sequence due to a continuous replacement of unbounded or bleached ligands. This allows obtaining a high-density number of molecular trajectories by (1) extracting the spatial coordinates of the fluorescent ligands along the time and (2) connecting all localized molecules frame after frame to reconstruct molecular trajectories.

Quantification of AMPAR content in nanodomains. The number of AMPARs per each nanodomain was estimated from dSTORM super-resolved images of endogenous GluA2 using a custom-made analysis module operating inside MetaMorph software. For each recorded cell, single AMPARs were identified using wavelet segmentation and Gaussian fitting as isotropic and isolated objects of 40 nm in diameter. Isolated single AMPARs were differentiated from nanoclusters resulting from the high spatial resolution provided by dSTORM technique. The histogram and median of the integrated intensity of each individual AMPAR per cell were then computed. This links the intensity distribution of one tetrameric structure, in function of the ratio of immunolabelled GluA2 with the other non-labelled AMPARs subunits. Synaptic nanodomains were finally determined using wavelet segmentation and the number of receptors per cluster was assessed by dividing the cluster's total intensity by the median intensity of the identified isolated AMPARs.

Quantification of AMPAR surface density using dSTORM. The surface density of AMPARs per μm^2 was estimated from dSTORM super-resolved images of endogenous GluA2 using a custom-made analysis module operating inside MetaMorph software. For each recorded cell, single AMPARs were identified and the median of the integrated intensity of individual receptors was calculated as previously described. Dendritic and synaptic regions were identified by wavelet image segmentation of the labelled GluA2-containing AMPARs. The corresponding binary mask was used to sort single particle data analysis to specific synaptic and dendritic regions. The surface density of AMPARs for each region was then determined by dividing the global intensity of localizations by the median intensity of the identified isolated AMPARs in function of the ROI area.

Statistics. Statistical values are gives as medians IQR or mean ± SEM. Statistical significances were performed using GraphPad Prism software (San Diego, CA). Used statistical test are specified in the text in function to the number of comparison and the result of the normality test. Normally distributed data sets were tested by Student's unpaired t-test for two independent groups unless stated otherwise. Non-Gaussian distribution datasets were tested by Mann-Whitney U test. Multiple-comparisons were performed by One-way ANOVA using Dunnett's *post hoc* multiple comparison test or by Krustal-Wallis test. Indications of significances correspond to p values <0.05(*), $p<0.01$(**), $p<0.001$(***), and $p<0.0001$(****).

Results

Characterization of the acute manipulation of endogenous Shisa6

The effect of acute manipulation of the endogenous Shisa6 levels were first determined using wide field microscopy (fig.8). This approach was used to determine the subcellular expression of Shisa6 and the impact of this protein on spine morphology development. Dissociated hippocampal neurons were transfected with EGFP::Shisa6 to overexpress the protein or with shRNA::Shisa6 to downregulate its expression, knockdown (*KD*). The specificity of Shisa6 *KD* was determined by a rescue experiment using EGFP::Shisa6::Rescue. Transfected cells were fixed at 10-14 or 21 *DIV* and double stained for endogenous GluA2-containing AMPARs in combination with overexpressed EGFP::Shisa6 or endogenous PSD-95 (fig. 8A). For a complete characterization, recordings were systematically performed between proximal (50-120 μm from cell body) and distal (220-290 μm from cell body) dendritic regions. Dendritic spines were isolated by wavelet segmentation of the EGFP signal, creating segmented objects corresponding to the isolated synapses. All the analysis was performed in synapses containing a granular co-enrichment of the GluA2 and EGFP::Shisa6 or PSD-95 signals. The major and minor axis of all segmented objects were calculated and used to extract spine aspect ratio. This ratio was used as a simple morphological estimation to discern between immature filopodia (aspect ratio<0.5) and mushroom-like spines (aspect ratio>0.5). Segmented objects were additionally used to extract the EGFP::Shisa6 fluorescence signal within the delimited region.

The fluorescence intensity of EGFP::Shisa6 surface labelling was analysed to characterize the synaptic expression of Shisa6 (fig. 8B). A preferential accumulation of overexpressed EGFP::Shisa6 was found in distal synaptic sites, as indicated by an increase of fluorescence intensity compared to proximal ones (Shisa6 overexpression Proximal = 3.3 ± 1.7; Shisa6 overexpression Distal = 4.4 ± 2.2, unpaired t-test, $p<0.001$). To ensure that this effect is not an artefact of Shisa6 overexpression, the fluorescence intensity of EGFP::Shisa6::Rescue in both distal and proximal synaptic regions was quantified. A small trend, although non-significant, to increased EGFP::Shisa6 fluorescence intensity is found in distal synaptic regions (Shisa6 rescue Proximal = 3.4 ± 1.3; Shisa6 rescue Distal = 3.9 ± 1.8, unpaired t-test, $p<0.15$). These preliminary results raise the possibility that Shisa6 might present a distal to proximal synaptic expression gradient.

Shisa9 is reported to impact cell morphology and spinogenesis indirectly by regulating the number of AMPARs at the cell surface (Khodosevich et al., 2014). To understand if Shisa6 influences spine morphology development, the endogenous levels of this proteins was manipulated during development (fig. 8C-D). Shisa6 *KD* impairs spine maturation at early developmental stages. This effect is independent of the distance to the soma (Proximal: Control = 0.6 IQR 0.5-0.7; Shisa6 *KD* = 0.4 IQR 0.2-0.6; Control = 0.5 IQR 0.5-0.7; Distal Shisa6 *KD* = 0.3 IQR 0.2-0.4). A similar impairment is seen in mature hippocampal neurons (21 DIV). Interestingly, the effect of Shisa6 *KD* at late developmental stages is more pronounced in distal dendrites (Proximal: Control: = 0.6 IQR 0.5-0.7; Shisa6 *KD* 0.5 IQR

0.3-0.6; Distal: Control = 0.6 IQR 0.5-0.7; Shisa6 *KD* = 0.4 IQR 0.3-0.6). This effect is specific for Shisa6 and not due to off-target effects of the shRNA since is reversed by a rescue experiment (Proximal: Control = 0.6 IQR 0.5-0.7; Shisa6 Rescue = 0.5 IQR 0.4-0.7; Distal: Control = 0.5 IQR 0.4-0.7; Shisa6 Rescue = 0.6 IQR 0.4-0.7). In agreement with an expression gradient for Shisa6, the rescue efficacy at 10-14 *DIV* is higher for distal dendrites than to proximal ones. Shisa6 overexpression increases the number of mushroom-like spines at distal dendrites during earlier developmental stages. Indeed, the median aspect ratio was increased when overexpressing this protein (Proximal: Control = 0.6 IQR 0.5-0.7; Shisa6 Rescue = 0.6 IQR 0.5-0.7; Distal: Control = 0.5 IQR 0.4-0.7; Shisa6 Rescue = 0.6 IQR 0.4-0.7). The effect of Shisa6 overexpression is exclusive to distal dendrites and to early developmental stages. Corroborating a restricted effect for Shisa6, no differences were seen between Shisa6 rescue and control littermates at late developmental stages. Thus, the acute manipulation of endogenous Shisa6 has a bidirectional impact in spine morphology development. This effect is more pronounced in distal dendritic regions and at early developmental stages.

Altogether these results suggest a preferential expression of Shisa6 in distal dendritic regions where it impacts spine morphology development. Indeed, wide field microscopy point out that EGFP::Shisa6 surface expression is enriched in distal dendritic spines. Corroborating this expression gradient, the impact of Shisa6 overexpression in spine morphology is exclusive to distal dendrites. Similarly, the efficacy of Shisa6 rescue is higher for these regions. Interestingly, the effect of Shisa6 in distal dendrites appears to be temporal restricted, since no differences are seen at later developmental stages. Surprisingly, Shisa6 *KD* decreased the median aspect ratio independently of the distance to the soma. A decrease in the number of mushroom-like spines is also seen in mature hippocampal neurons, suggesting a predominant impairment along the development. However, at late developmental stages, the effect caused by Shisa6 *KD* is more pronounced in distal dendritic regions.

Figure 8 – Characterization of the acute manipulation of endogenous Shisa6. A) Transfected hippocampal neurons double stained for endogenous GluA2-containing AMPARs in combination with overexpressed EGFP::Shisa6 (Overexpression and Rescue experiments) or endogenous PSD-95 (Shisa6 KD and control littermates). GluA2 (red) and EGFP-Shisa6 surface labelling (Alexa 568, green). For illustration proposes the EGFP signal is not shown. Recordings were systematically performed between proximal (50-120 μm from cell body) and distal (220-290 μm) regions. Spines were isolated by segmentation of the EGFP signal and analysis performed in synapses containing a co-enrichment of the GluA2 and EGFP::Shisa6 or PSD-95 signals (white arrows). The major and minor axes were computed to determine the aspect ratio of the segmented object. **B)** Fluorescence intensity quantification for GFP::Shisa6 surface labelling for 10-14 DIV aged neurons. Shisa6 overexpression Proximal: 3.36 ± 1.77 (n=19); Shisa6 overexpression Distal: 4.4 ± 2.27 (n=19), unpaired t-test, $p<0.001$; Shisa6 rescue Proximal: 3.38 ± 1.27 (n=21); Shisa6 rescue Distal: 3.99 ± 1.84 (n=21), unpaired t-test, $p<0.148$. **C)** Quantification of aspect ratio for all isolated spines. Proximal analysis 10-14 DIV: Control = 0.597 IQR 0.46-0.75 (176 spines, n=20); Shisa6 KD = 0.394 IQR 0.26-0.58 (196 spines, n=20); Shisa6 overexpression = 0.597 IQR 0.49-0.74 (189 spines, n=19); Shisa6 rescue = 0.537 IQR 0.40-0.69 (298 spines, n=21), Krustal-Wallis test. Proximal analysis 21 DIV: Control= 0.608 IQR 0.45-0.74 (99 spines, n=9); Shisa6 KD = 0.521 IQR 0.35-0.65 (77 spines, n=6); Shisa6 overexpression = 0.528 IQR 0.42-0.77 (41 spines, n=3); Shisa6 rescue = 0.598 IQR 0.51-0.72 (164 spines, n=9), Krustal-Wallis test. **D)** Distal analysis 10-14 DIV: Control= 0.539 IQR 0.39-0.69 (322 spines, n=20); Shisa6 KD = 0.333 IQR 0.21-0.47 (153 spines, n=20); Shisa6 overexpression = 0.578 IQR 0.46-0.73 (291 spines, n=19); Shisa6 rescue = 0.570 IQR 0.47-0.69 (267 spines, n=21), Krustal-Wallis test. Distal analysis 21 DIV: Control=: 0.598 IQR 0.49-0.71 (117 spines, n=9); Shisa6 KD = 0.382 IQR 0.27-0.58 (44 spines, n=6); Shisa6 overexpression = 0.499 IQR 0.40-0.67 (40 spines, n=3); Shisa6 rescue = 0.619 IQR 0.40-0.68 (144 spines, n=9), Krustal-Wallis test. Values represent the median aspect ratio determined from all spines analyzed (for each condition).

Figure in the next page

A Experimental Procedure

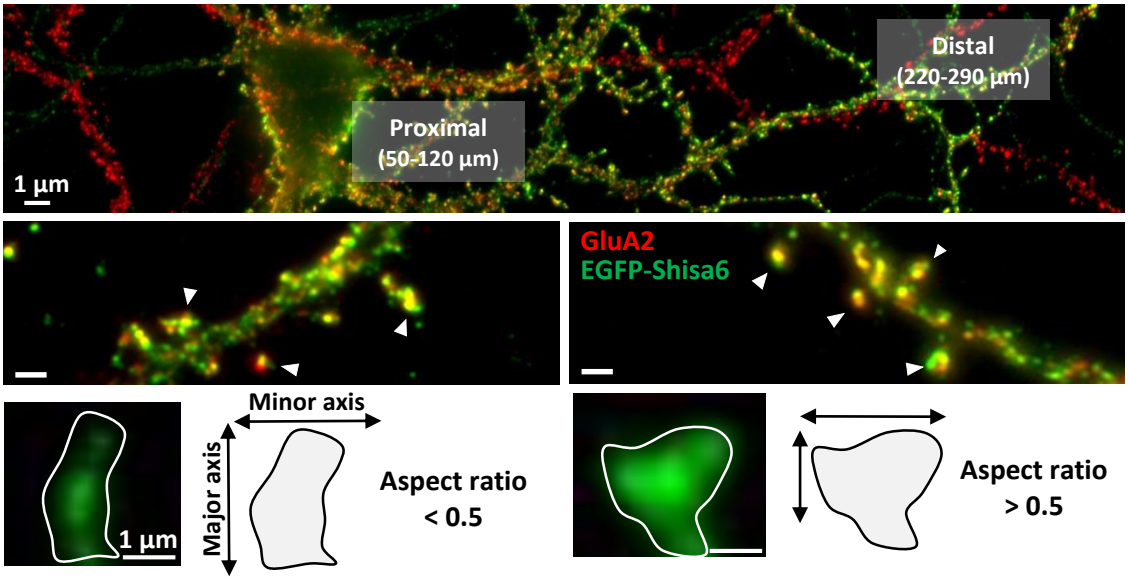

B GFP-Shisa6 surface labelling

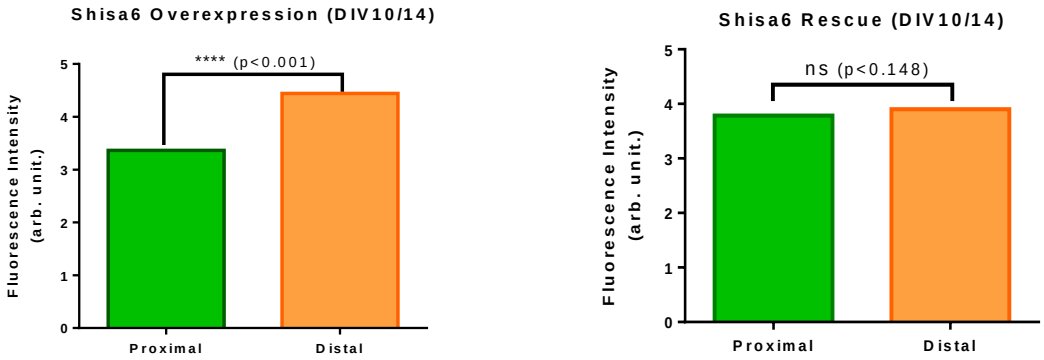

C Spine Morphology – Proximal Analysis

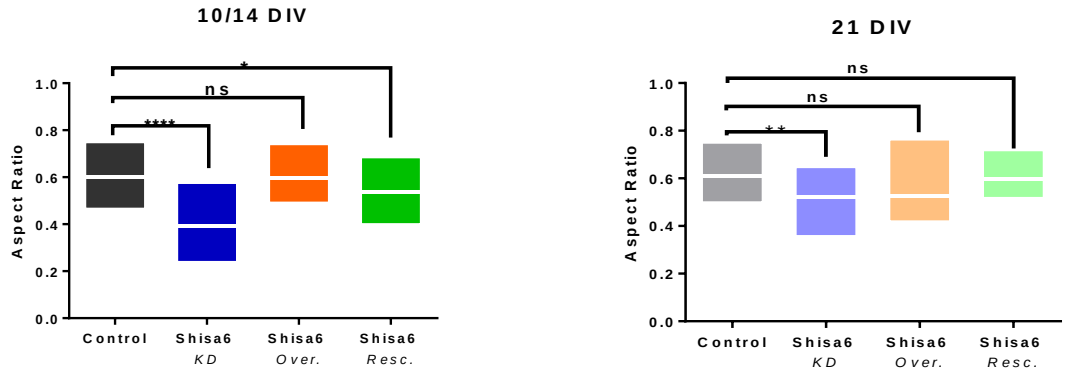

D Spine Morphology – Distal Analysis

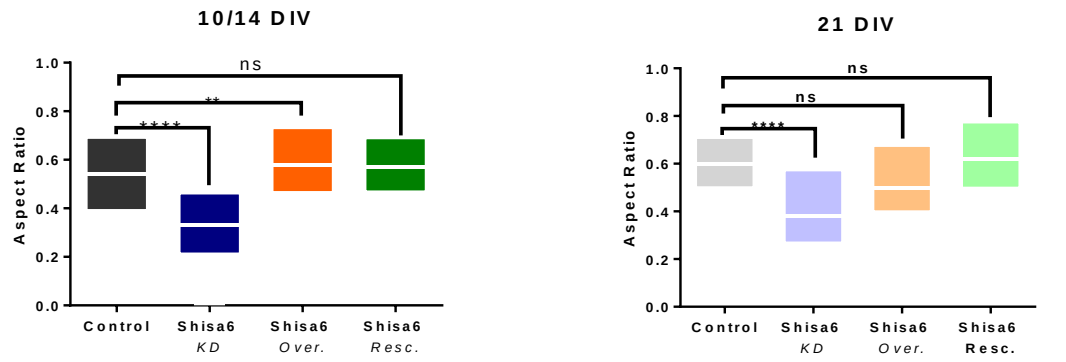

Shisa6 KO does not impact AMPAR nanoscale organization

A differential topological regulation of synaptic AMPARs was proposed, raising the possibility that synaptic composition can be distinct between proximal and distal dendrites (Andrásfalvy and Magee, 2001; Nicholson et al., 2006). If Shisa6 has a synaptic expression gradient, this protein could modulate AMPAR properties differentially between these dendritic regions. It was described that AMPAR auxiliary proteins are able to promote receptor surface expression (Tomita et al., 2003; Rouach et al., 2005; Khodosevich et al., 2014). dSTORM was applied to understand if Shisa6 promotes AMPAR surface expression differentially between proximal and distal dendrites (Fig. 9). Fixed hippocampal neurons derived from Shisa6 *KO* mice strains were live stained using antibodies directed to the extracellular domain of GluA2. Since the majority of the hippocampal AMPARs are composed by associations of GluA2/A1 or GluA2/A3, this allowed to determine the behavior of the overall population of surface receptors (Lu et al., 2009). Super-resolved images were obtained using appropriate algorithms that combines the accumulation of localization for GluA2-containing AMPARs from different diffraction-limited images acquired along 20,000 frames. To further characterize the distal to proximal expression gradient of Shisa6, recordings were performed as described above.

The total number of AMPARs inside the synapse and in dendritic regions was estimated from super-resolved images by dividing the total number of the single-molecule detection by the median intensity of isolated receptors (fig.9A). Shisa6 KO does not change the total number of surface AMPARs in either proximal or distal dendrites (Proximal: *Wild-type* = 40.6 IQR 29.7-58.3, Shisa6 *KO* = 33.6 IQR 26.2-40.1, Mann-Whitney test, p=0.1; Distal: *Wild-type* = 35.9 IQR 24.6-47.9, Shisa6 *KO* = 38.9 IQR 30.8-61.3, Mann-Whitney test, p=0.2; Fig.9B). Moreover, Shisa6 *KO* left unchanged the total number of surface AMPARs inside the synapse compared to control littermates (fig.9C). No differences were detected in the average number of synaptic AMPARs between proximal and distal dendritic regions (Proximal: *Wild-type* = 63.59 IQR 51.96-70.15, Shisa6 *KO* = 50.46 IQR 40.49-71.13, Mann-Whitney test, p=0.38; Distal: *Wild-type* = 46.72 IQR 28.16-63.69, Shisa6 *KO* = 49.56 IQR 37.98-79.29, Mann-Whitney test, p=0.21). Furthermore, Shisa6 *KO* does not impact AMPAR surface expression. As expected, the number of AMPARs is enriched at the synapses compared to extrasynaptic regions for both proximal and distal recordings.

Since Shisa6 interacts with the scaffold PSD-95 through its PDZ ligand-binding motif, it is potentially able to regulate AMPAR synaptic stabilization. As consequence of its synaptic expression gradient, the role of this protein can be differential between proximal and distal dendritic regions. Even though it does not change the overall number of AMPARs at the synapses, Shisa6 might still impact their nanoscale organization. It is described that synaptic AMPARs are organized in nanodomains containing around 20-25 receptors (MacGillavry et al., 2013; Nair et al., 2013). dSTORM was performed to study if Shisa6 *KO* impacts (1) nanodomains content and (2) the number of synaptic nanodomains. To know if Shisa6 regulates the number of AMPARs per nanodomain, the cluster's total intensity was

divided by the median intensity of isolated receptors for each super-resolved image. This data was then filtered to determine the number of receptors organized in nanodomains exclusively at mushroom shaped spines in both proximal and distal dendrites (fig.10A). The estimated number of AMPARs per nanodomain is not changed between Shisa6 *KO* and control littermates. Indeed, the nanodomain content is left unchanged by Shisa6 *KO* to a similar extent between proximal and distal regions (*Proximal:* Wild-type= 17.79 ± 1.07, Shisa6 KO= 17.09 ± 1.0, Mann-Whitney test, p=0.7; Distal: *Wild-type*= 17.08 ± 1.07; Shisa6 *KO*= 17.7 ± 0.76; Mann-Whitney test, p=0.312; fig 10B). The total number of nanodomains per spine was estimated by counting the number of clusters inside the synapse. Cumulative frequency distribution of the number of nanodomains per spine for both proximal and distal dendrites is represented in fig.10B. No differences are seen in function to the distance to the soma between Shisa6 *KO* and control littermates (Proximal: *Wild-type*= 3.57 ± 0.25, Shisa6 *KO*= 3.88 ± 0.22, Mann-Whitney test, p=0.3939; Distal: *Wild-type*= 3.99 ± 0.17, Shisa6 *KO*= 3.87 ± 0.18, Mann-Whitney test, p=0.6167). These numbers are higher than those previously reported (≈2 nanodomains per spine), possibility due to the use of mice hippocampal neurons (Nair et al., 2013). Collectively these data indicates that Shisa6 *KO* does not change the total number of surface AMPAR in extrasynaptic or synaptic regions. This effect is also not associated with major changes in their subsynaptic organization at the nanoscale level.

Shisa6 KO does not impact AMPAR surface mobility

Because Shisa6 is synaptically localized, is interacting with AMPARs, and can potentially bind PDZ-containing scaffold proteins, it might affect receptor mobility at the neuronal membrane. uPAINT was performed as a high-density single particle tracking technique to explore the role of Shisa6 in AMPAR surface mobility. Fluorescently labelled antibodies directed to the extracellular domain of GluA2 were used to randomly label surface AMPAR on dissociated hippocampal neurons derived from Shisa6 *KO* mice strains (fig.11). Proximal and distal recordings were systematically performed to understand if the synaptic expression gradient of Shisa6 is translated in differences on receptor mobility between these regions. To determine the impact of Shisa6 in the overall mobility of GluA2-containing AMPARs, single molecular trajectories derived from both dendritic and synaptic regions were considered. This allowed to computing the average distribution of the instantaneous diffusion coefficients (D) for both proximal and distal recordings. Globally, the mobility of endogenous AMPARs is not changed by Shisa6 *KO* in both proximal and distal dendrites (fig.11A-B). This was confirmed by accessing the cumulative variation of AMPARs inside the mobile fraction (D> -1.6 μm^2) between each conditions. Indeed, no differences in the pool of mobile AMPARs are seen between Shisa6 *KO* and control littermates for proximal regions (Shisa6 *KO* = 47.3 ± 2.2, *Wild-type* = 42.5 ± 4.7, unpaired t-test, p=0.4). Similarly, the pool of mobile AMPARs for distal regions is also unchanged by Shisa6 *KO* (Shisa6 *KO* = 52.0 ± 5.0, *Wild-type* = 43.5 ± 3.8, unpaired t-test, p=0.2). Thus, the absence of Shisa6 does not directly impact AMPAR surface mobility in both proximal and distal dendrites of mice hippocampal neurons.

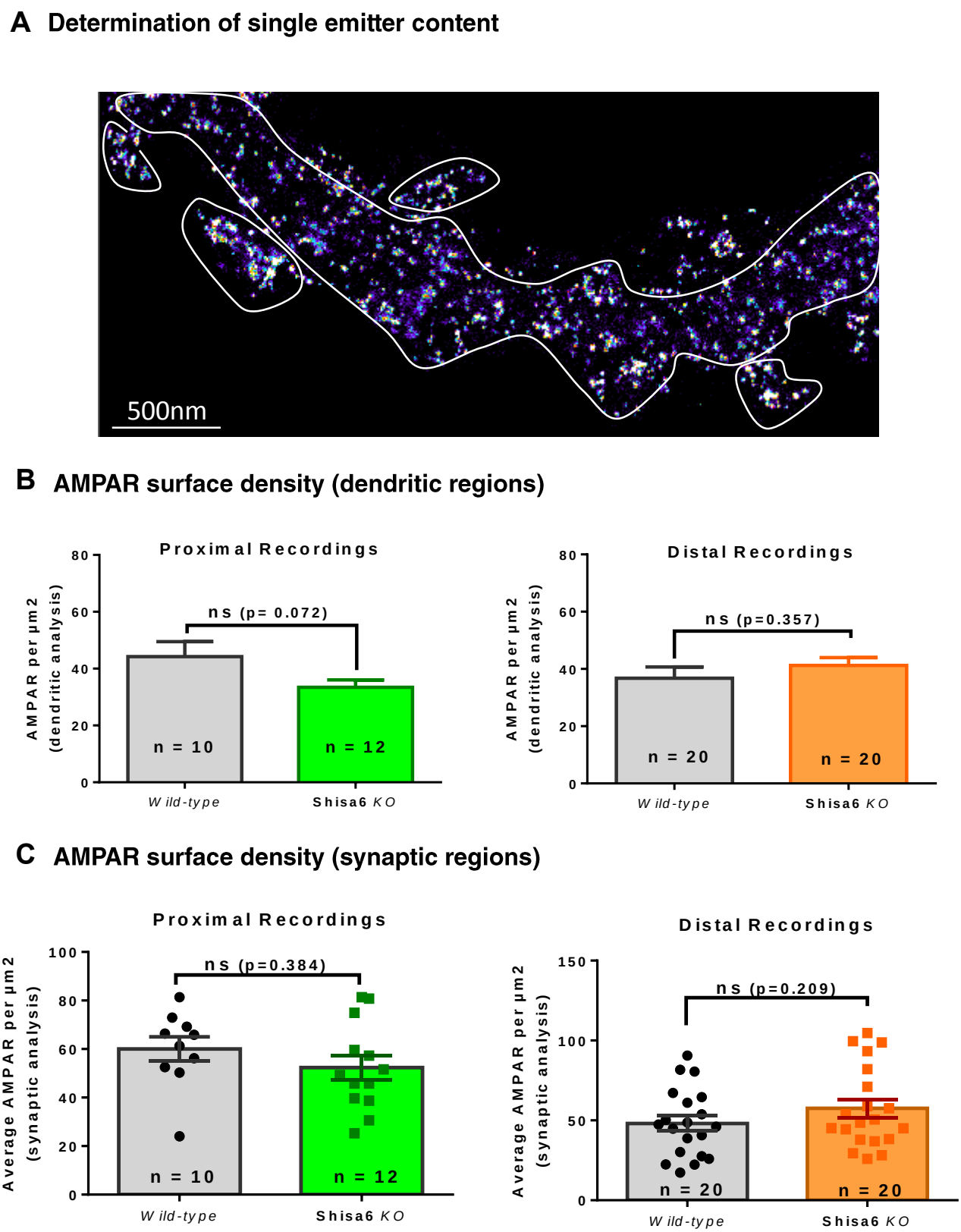

Figure 9 – Shisa6 KO does not change the total number of AMPARs in both dendritic and synaptic regions: **A)** Super-resolved image of dendritic and synaptic regions. **B)** Quantification of AMPARs per μm^2 in dendritic regions from both proximal and distal recordings. Proximal wild-type = 40.6 IQR 29.7-58.3 (n=10), Proximal Shisa6 KO= 33.6 IQR 26.2-40.1 (n=12), Mann-Whitney test, p=0.071; Distal wild-type = 35.9 IQR 25.6-47.9 (n=20), Distal Shisa6 KO = 41.22 ± 2.731 (n=20), unpaired t-test, p=0.357). **C)** Quantification of the average number of AMPAR inside the synapse. Proximal *Wild-type* = 63.59 IQR 51.96-70.15 (n=10), Proximal Shisa6 *KO* 50.46 IQR 40.49-71.13 (n=12), Mann-Whitney test, p=0.384; Distal *Wild-type* = 46.72 IQR 28.16-63.69 (n=20), Distal Shisa6 *KO* = 49.56 IQR 37.98-79.29 (n=20), unpaired t-test, p=0.209.

A dSTORM imaging

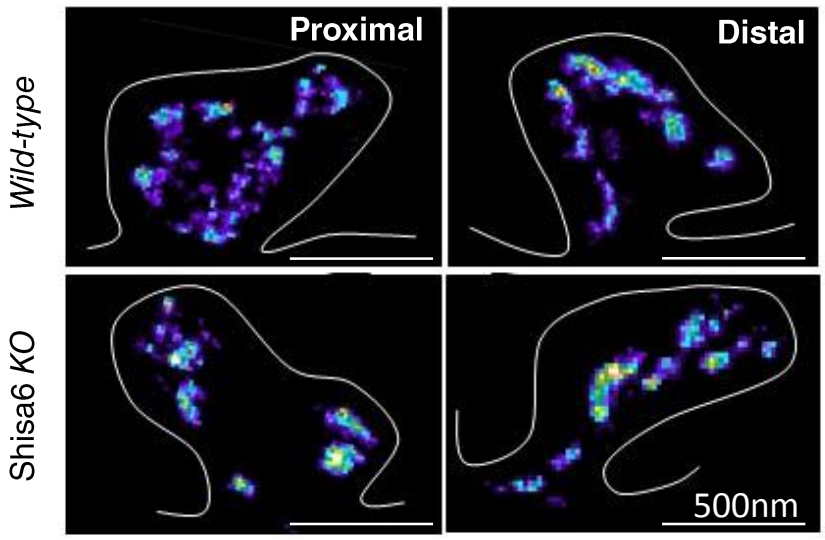

B Nanodomain characteristics

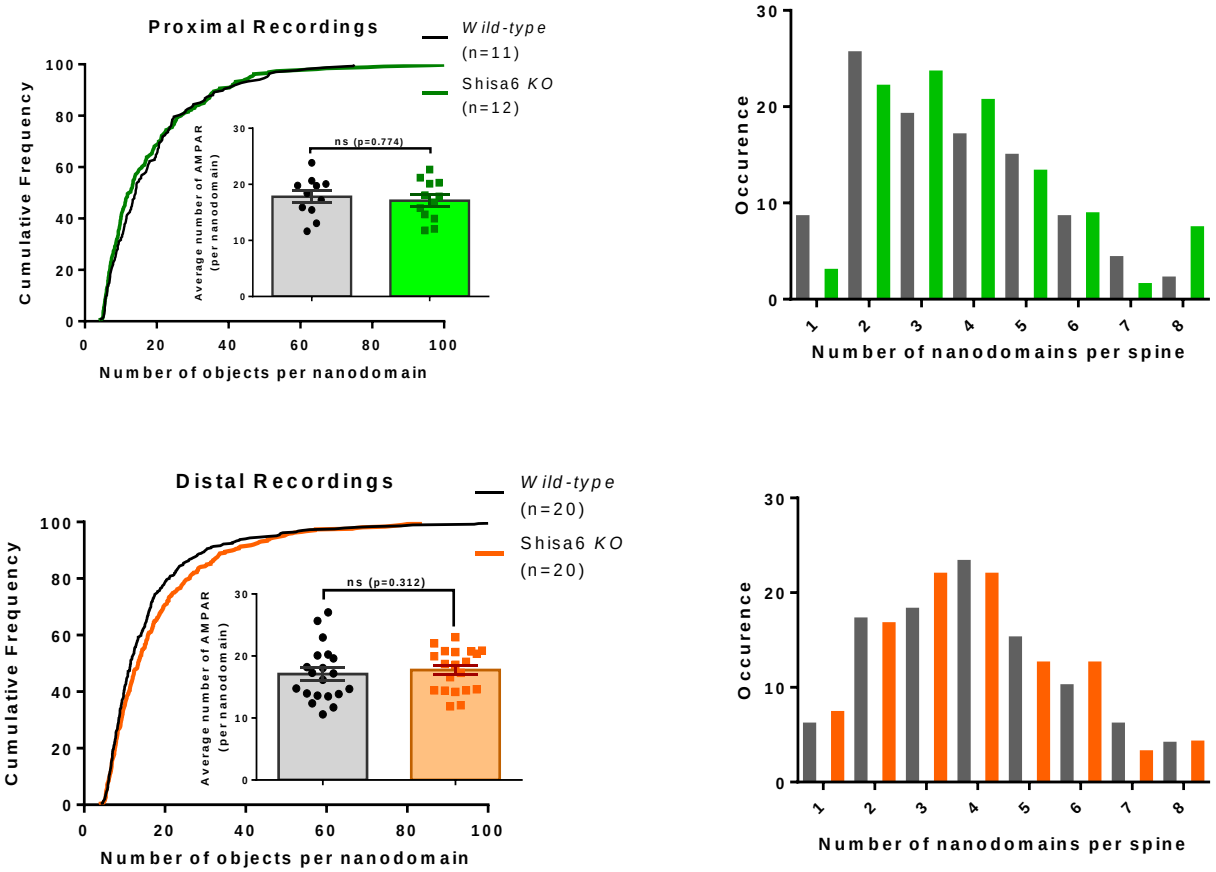

Figure 10 – Shisa6 *KO* does not impact the AMPAR nanoscale organization: A) Super-resolved intensity images of GluA2-containing AMPARs in dendritic spines obtained by dSTORM on mice hippocampal neurons. Proximal (50-120 µm from the soma) and distal (220–290 µm from the soma) recordings. **B)** *Left panels:* Cumulative distribution and, in the insert, average number of AMPARs per nanodomain for proximal (top) and distal (bottom) recordings. The number of AMPARs per nanodomain was estimated by dividing the cluster's total intensity by the median intensity of isolated receptors. Receptor content per nanodomain in proximal regions: *Wild-type* = 17.79 ± 1.07, n=11; Shisa6 *KO* = 17.09 ± 1.0, n=12; Mann-Whitney test, p=0.774; and in distal regions: *Wild-type* = 17.08 ± 1.07 (n=20), Shisa6 *KO* = 17.7 ± 0.76 (n=20), Mann-Whitney test, p=0.312. *Right panels:* Cumulative frequency distribution of the number of nanodomains per spine in proximal regions: *Wild-type*= 3.57 ± 0.25 (n=11), Shisa6 *KO* = 3.88 ± 0.22 (n=12), Mann-Whitney test, p=0.394; and in distal regions: *Wild-type* = 3.99 ± 0.17 (n=20), Shisa6 *KO* = 3.87 ± 0.18 (n=20), Mann-Whitney test, p=0.617.

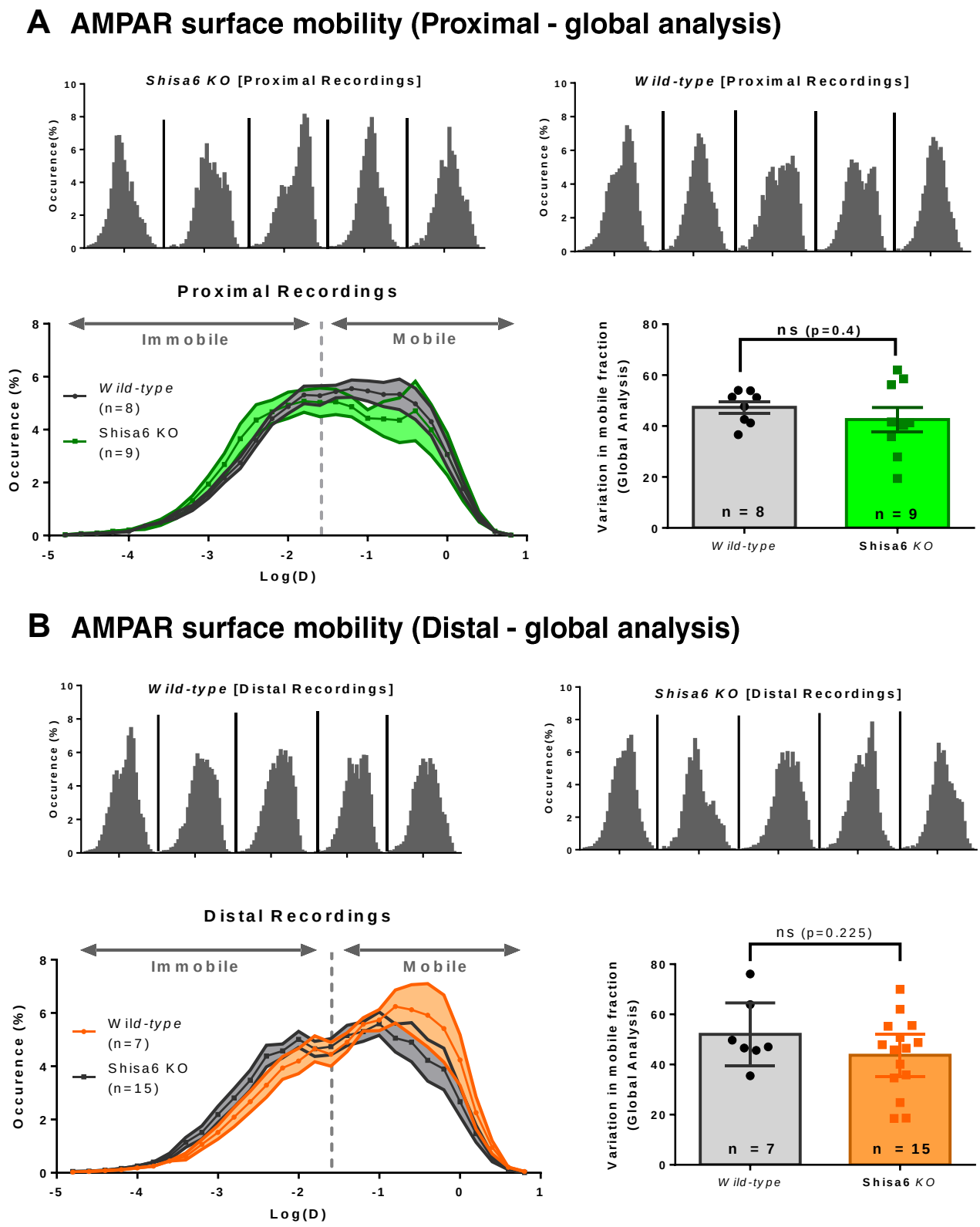

Figure 11 – Shisa6 *KO* does not impact the surface mobility of endogenous GluA2-containing AMPARs: uPAINT microscopy was performed using antibodies coupled to ATTO647N directed against the extracellular region of GluA2-containing AMPARs present in the neuronal cell membrane. **A)** *(Top panel)*: cell-to-cell variability. *(Bottom panel) Left:* Average distribution of D for molecular trajectories obtained by uPAINT from whole dendritic segments of proximal recordings. Error area indicates cell-to-cell variability; *Right:* Cumulative variation of AMPARs in the mobile fraction (dashed line: D> -1.6 µm2/s). The frequency distribution of the population of AMPARs present in the mobile fraction was summed and their variability is shown. Shisa6 *KO* = 47.34 ± 2, 29 (n=9), *Wild-type* = 42.58 ± 4.75 (n=8), unpaired t-test, p=0.4. **B)** *(Top panel)*: cell-to-cell variability. *(Bottom panel) Distal analysis:* Shisa6 *KO* = 52.06 ± 5. 09 (n=7), *Wild-type* = 43,568 ± 3.89 (n=15), unpaired t-test, p=0.225.

Shisa6 EVTV increases AMPAR surface mobility in distal synaptic regions

To exclude that the previous absence of effects on AMPAR surface mobility is due to compensatory mechanisms of the global Shisa6 *KO*, uPAINT microscopy was performed with acute manipulation of endogenous Shisa6 levels (fig.12A). Dissociated hippocampal neurons were overexpressed with EGFP::Shisa6 and knock-down (KD) with shRNA::Shisa6. A mutant Shisa6 lacking the putative PDZ domain-binding motif (EVTV) was additionally used to determine the dependence of the interaction with intracellular scaffolding elements. EGFP was expressed either alone (control) or in combination with all the conditions to identify dendritic spines. Reconnecting the localization of individual GluA2 made possible to compute trajectories of endogenous AMPARs along the neuronal surface for both dendritic and synaptic regions (fig.12B). Proximal and distal recordings were systematically performed as described above to understand if the synaptic expression gradient of Shisa6 is translated in differences on receptor mobility.

The impact of Shisa6 acute manipulation in AMPAR surface mobility was first evaluated considering dendritic and synaptic trajectories (fig.12C). For proximal regions, the acute manipulation of Shisa6 does not alter the number of mobile AMPARs compared to control littermates (Control = 41.0 ± 4.0; Shisa6 *KD* = 47.2 ±5.1; Shisa6 overexpression = 43.6 ± 4.5; Shisa6 EVTV = 53.3 ± 4.7; One-way ANOVA with Dunett's multiple comparison *post hoc* test). Similarly, no differences are seen between Shisa6 overexpression, Shisa6 *KD*, and control littermates for distal dendrites. Surprisingly, overexpression of Shisa6 EVTV increases the surface mobility of AMPARs (Control = 41.1 ± 2.8; Shisa6 *KD* = 36.6 ± 3.5; Shisa6 overexpression = 43.0 ± 3.5; Shisa6 EVTV = 61.2 ± 4.8; One-way ANOVA with Dunett's multiple comparison *post hoc* test). If the analysis is restricted to synaptic trajectories, a similar effect of Shisa6 EVTV overexpression in the pool of mobile AMPARs for distal regions is seen (Control: 42.9 ± 3.3; Shisa6 *KD*: 38.7 ± 2.9; Shisa6 overexpression: 36.3 ± 4.9; Shisa6 EVTV: 62.6 ± 6.0; One-way ANOVA with Dunett's multiple comparison *post hoc* test; fig.12D *left panel*). This indicates that the acute manipulation here performed directly impacts the diffusional properties of synaptic AMPARs.

To understand if Shisa6 confines endogenous AMPARs at synaptic sites, the MSD was determined for trajectories restricted to synaptic regions (fig.12D *right panel)*. MSD is commonly used to determine the area explored by a molecule over the time, considering the cell membrane as a homogenous two dimensional plane (Triller and Choquet, 2008). Shisa6::EVTV overexpression decreases the synaptic confinement (i.e. increases mobility) of GluA2-containing AMPARs in distal dendrites as evidenced by the increase of the plateau reached by the MSD curve compared to control littermates (Shisa6 EVTV MSD plateau = 0.05 ± 0.02 μm^2 at t=1s; Shisa6 overexpression MSD plateau= 0.01 ± 0.01 μm^2 at t=1s; Shisa6 KD MSD plateau = 0.01 ± 0.002 μm^2 at t=1s; Control MSD plateau = 0.02 ± 0.002 μm^2 at t=1s; fig.12D *right panel*). If the same analysis is restricted to proximal regions, the effect of Shisa6::EVTV overexpression in

AMPARs synaptic confinement is abolished (Shisa6 EVTV MSD plateau = 0.02 ± 0.01 at t=1s; Shisa6 overexpression MSD plateau= 0.01 ± 0.011 μm^2 at t=1s; Shisa6 *KD* MSD plateau = 0.01 ± 0.003 μm^2 at t=1s; Control MSD plateau = 0.03 ± 0.01 μm^2 at t=1s). No differences on the MSD are seen between Shisa6 overexpression, Shisa6 *KD,* and control littermates for both proximal and distal dendritic regions.

Altogether these results suggest a complex relationship between Shisa6 and AMPAR. Shisa6 overexpression and *KD* does not impact AMPAR surface mobility. However, Shisa6::EVTV overexpression decreases AMPAR synaptic clustering and increases surface mobility exclusively in distal dendritic regions. This corroborates that the effect of Shisa6 on AMPAR surface mobility is dependent on interactions between its PDZ ligand-binding motif and synaptic scaffolding elements. This effect is exclusive to distal dendrites, in agreement with a synaptic expression gradient for this protein. Thus, Shisa6 impacts AMPAR surface mobility differentially between proximal and distal dendritic regions due to direct interactions with scaffolding proteins.

Surface mobility of GFP::Shisa6 is not different between proximal and distal synaptic regions

After characterizing the role of Shisa6 in AMPAR lateral diffusion, uPAINT was used to understand if this auxiliary protein has a different surface mobility between proximal and distal dendrites. If Shisa6 acts preferentially in distal synaptic regions, then a decrease of its surface mobility should be expected as similar to what was seen for endogenous AMPARs. uPAINT was performed using fluorescently labelled nanobodies specific to the extracellular EGFP-tag of overexpressed Shisa6 on rat hippocampal cultures (fig.13). Dissociated hippocampal neurons were overexpressed with EGFP::Shisa6 and EGFP::Shisa6::EVTV (fig.13A). The mutant Shisa6 EVTV was used as an intrinsic control for Shisa6 overexpression. Since Shisa6 EVTV is not able to interact with intracellular scaffolding elements, its surface mobility should be (1) higher compared to EGFP::Shisa6 and (2) similar between distal and proximal dendrites. This allows to exclude that differences on surface mobility for EGFP::Shisa6 between these dendritic regions are due to an artefact of its overexpression. Reconnecting the localization of individual EGFP-Shisa6 made possible to compute trajectories of both conditions for extrasynaptic and synaptic regions (fig.13B).

The global surface mobility of EGFP::Shisa6 was first determined considering dendritic and synaptic cells trajectories (fig. 13C). No significative differences are found on the mobile pool of overexpressed EGFP::Shisa6 between proximal and distal dendrites (Proximal recordings = 50.2 ± 2.7; Distal Recordings = 54.7 ± 4.7; unpaired t-test, p=0.4). As expected, EGFP::Shisa6::EVTV overexpression has a similar surface mobility between both regions (Proximal recordings = 51.2 ± 2.5; Distal Recordings = 52.5 ± 3.3; unpaired t-test, p= 0.8). Considering that the role of Shisa6 can be preferentially synaptic, an analysis restricted to synaptic trajectories was then performed (fig.13D *right panel)*. Similarly, no differences on the mobile pool of overexpressed EGFP::Shisa6 are seen

between both dendritic regions (Proximal recordings = 51.5 ± 3.04; Distal Recordings = 51.1 ± 4.5; unpaired t-test, p= 0.9). A similar behavior is seen for EGFP::Shisa6::EVTV. To determine the area explored by EGFP::Shisa6 at the synapse, MSD analysis was performed for trajectories restricted to synaptic regions (fig.13D *left panel)*. As expected, no differences on the MSD plateau was seen for EGFP::Shisa6::EVTV overexpression between proximal and distal dendritic regions (Proximal recordings MSD plateau = 0.06 ± 0.4 μm² at t=0.5s; Distal Recordings MSD plateau = 0.05 ± 0.009 μm² at t=0.5s). In agreement with the previous set of results, no major differences on EGFP::Shisa6 MSD plateau are seen (Proximal recordings MSD plateau= 0.05 ± 0.009 μm2 at t = 0.5s; Distal Recordings MSD plateau= 0.03 ± 0.009 μm2 at t = 0.5s).

Altogether, these data indicates that surface mobility of GFP::Shisa6 is not different between proximal and distal dendritic regions. However, there are some intriguing results: (1) the pool of mobile EGFP::Shisa6 is similar between global and synaptic analysis; (2) assuming that Shisa6 is stabilizing AMPARs at the synapse, we expected its decreased at synaptic regions; (3) no differences in surface mobility were found between EGFP::Shisa6 and EGFP::Shisa6::EVTV (4) the MSD values obtained for EGFP::Shisa6 are higher compared to what was obtained when tracking endogenous AMPARs (compare fig. 12D and 13D). Interestingly, only the MSD values obtained from GluA2 trajectories of Shisa6 EVTV experiments are similar to the ones found for EGFP::Shisa6. All of the above could be explained by the fact that Shisa6 overexpression generates a greater surface population that not interacts with AMPARs. Furthermore, the pool of mobile Shisa6 that does not anchors AMPARs at the synapse might be preferentially tracked. This would justify why all the results obtained for EGFP::Shisa6 and EGFP::Shisa6::EVTV conditions are similar independently of the distance to the soma. This idea is also supported by a similar synaptic confinement of Shisa6 EVTV/GluA2 trajectories and overexpressed GFP::Shisa6. Thus, the differences in Shisa6 surface mobility between proximal and distal synaptic regions can be blunted under these experimental conditions.

Figure 12 – Shisa6 regulates the surface mobility of GluA2-containing AMPARs in rat hippocampal cultures: A) uPAINT microscopy was performed using antibodies directed to the extracellular domain of GluA2 on dissociated rat hippocampal neurons. Endogenous Shisa6 levels were acutely manipulated by overexpression of Flag::Shisa6 or EGFP::Shisa6EVTV and *KD* with shRNA::Shisa6. **B)** Super-resolved images of GluA2-containing AMPARs. Each super-resolved image represents individual trajectories lasting longer than 8 frames, obtained by overaccumulation of 4,000 images acquired with uPAINT technique. **C)** *(Left panel*) Cumulative variation of AMPARs present in the mobile fraction (D> -1.6 μm2/s) for both dendritic and synaptic regions. Proximal recordings: Control = 41.03 ± 4.08 (n=9); Shisa6 *KD* = 47.27 ± 5.18 (n=10); Shisa6 overexpression = 43.62 ± 4.55 (n=11); Shisa6 EVTV = 53.39 ± 4.76 (n=7); One-way ANOVA with Dunnett's multiple comparison post hoc test. Distal recordings: Control = 41.10 ± 2.89 (n=17); Shisa6 *KD* = 36.68 ± 3.55 (n=13); Shisa6 overexpression = 43.06 ± 3.56 (n=11); Shisa6 EVTV = 61.22 ± 4.82 (n=8); One-way ANOVA with Dunnett's multiple comparison post hoc test. **D)** *(Left panel)* Average distribution of instantaneous diffusion coefficients for molecular trajectories obtained by uPAINT in synaptic region. Proximal recordings: Control = 46.48 ± 5.67 (n=9); Shisa6 *KD* = 52.03 ± 5.46 (n=10); Shisa6 overexpression = 46.93 ± 8.70 (n= 11); Shisa6 EVTV = 61.54 ± 5.89 (n=7); One-way ANOVA with Dunnett's multiple comparison post hoc test). Distal recordings: Control = 42.91 ± 3.321 (n=17); Shisa6 *KD* = 38.72 ± 2.985 (n=13); Shisa6 overexpression = 36.33 ± 4.913 (n=11); Shisa6 EVTV = 62.60 ± 6.02 (n=8); One-way ANOVA with Dunnett's multiple comparison post hoc test. *(Right panel)* Graphical representation of MSD curves for control, Shisa6 KD and Shisa6 overexpression, and Shisa6 EVTV conditions. Error area indicates cell-to-cell variability. Proximal recordings: Shisa6 EVTV MSD plateau = 0.024 ± 0.01 μm² at t=1s; Shisa6 overexpression MSD plateau = 0.015 ± 0.01 μm² at t=1s; Shisa6 KD MSD plateau = 0.014 ± 0.004 μm² at t=1s; Control MSD plateau = 0.03 ± 0.01 μm² at t=1s. Distal Recordings: Shisa6 EVTV MSD plateau = 0.049 ± 0.018 μm² at t=1s; Shisa6 overexpression MSD plateau= 0.014 ± 0.01 μm² at t=1s; Shisa6 KD MSD plateau = 0.011 ± 0.002 μm² at t=1s; Control MSD plateau = 0.017 ± 0.002 μm² at t = 1s.

Figure in the next page

A Experimental Design

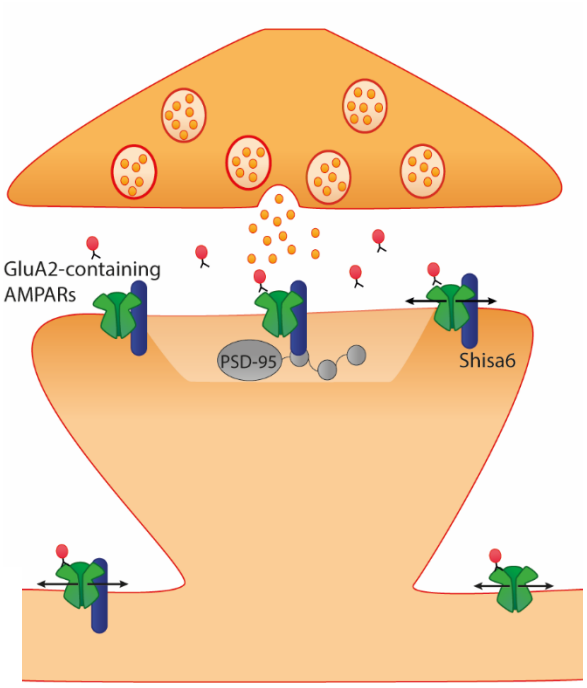

B uPAINT imaging

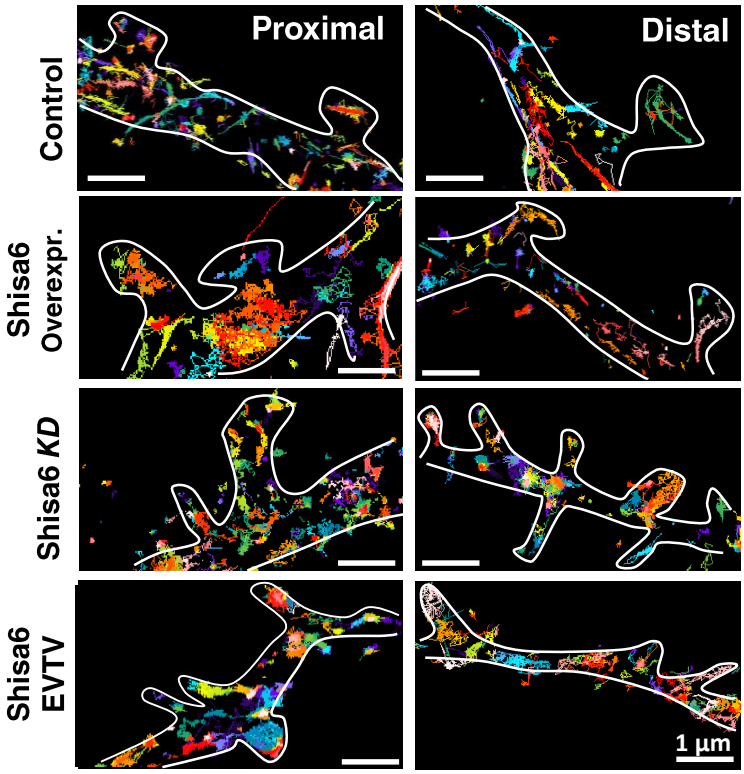

C AMPAR surface mobilty (Global Analysis)

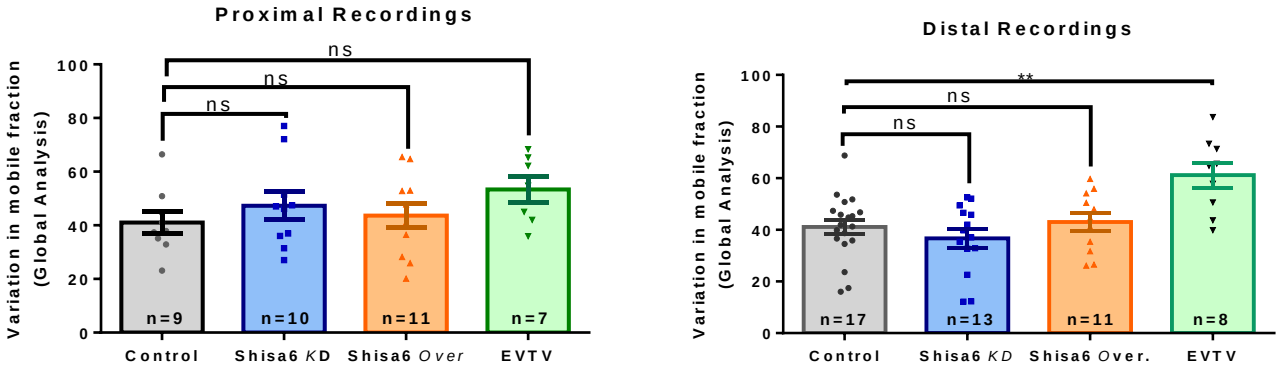

D AMPAR surface mobility (Synaptic Analysis)

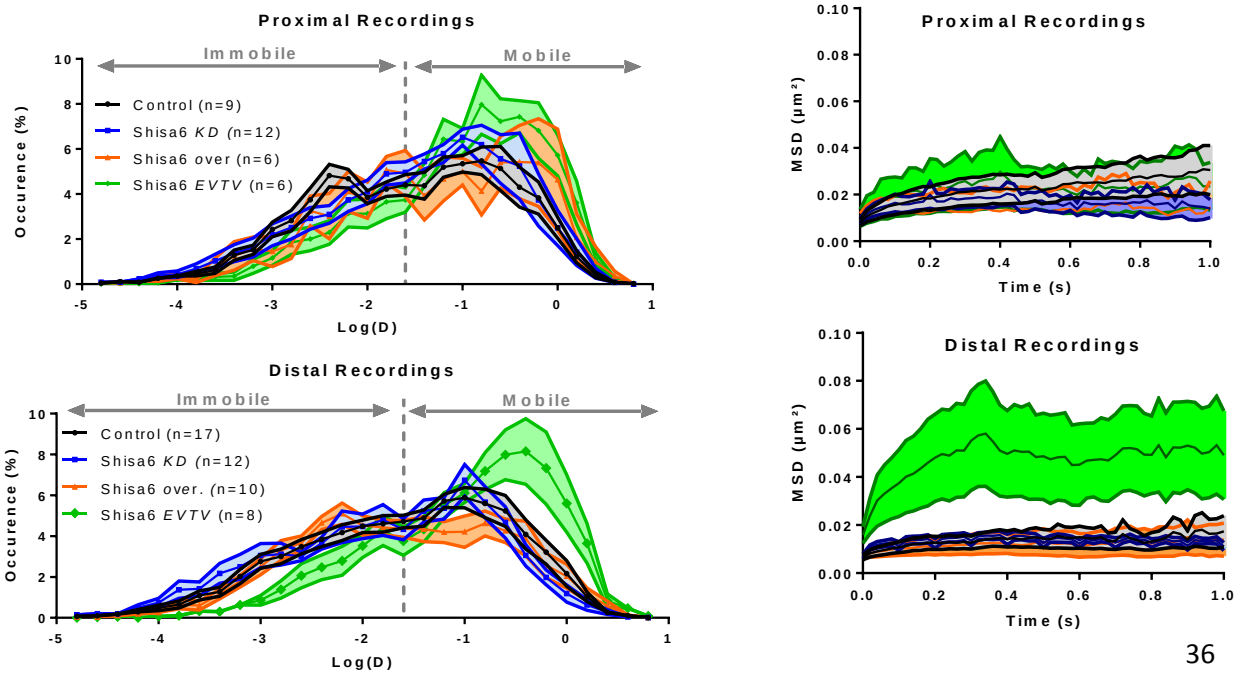

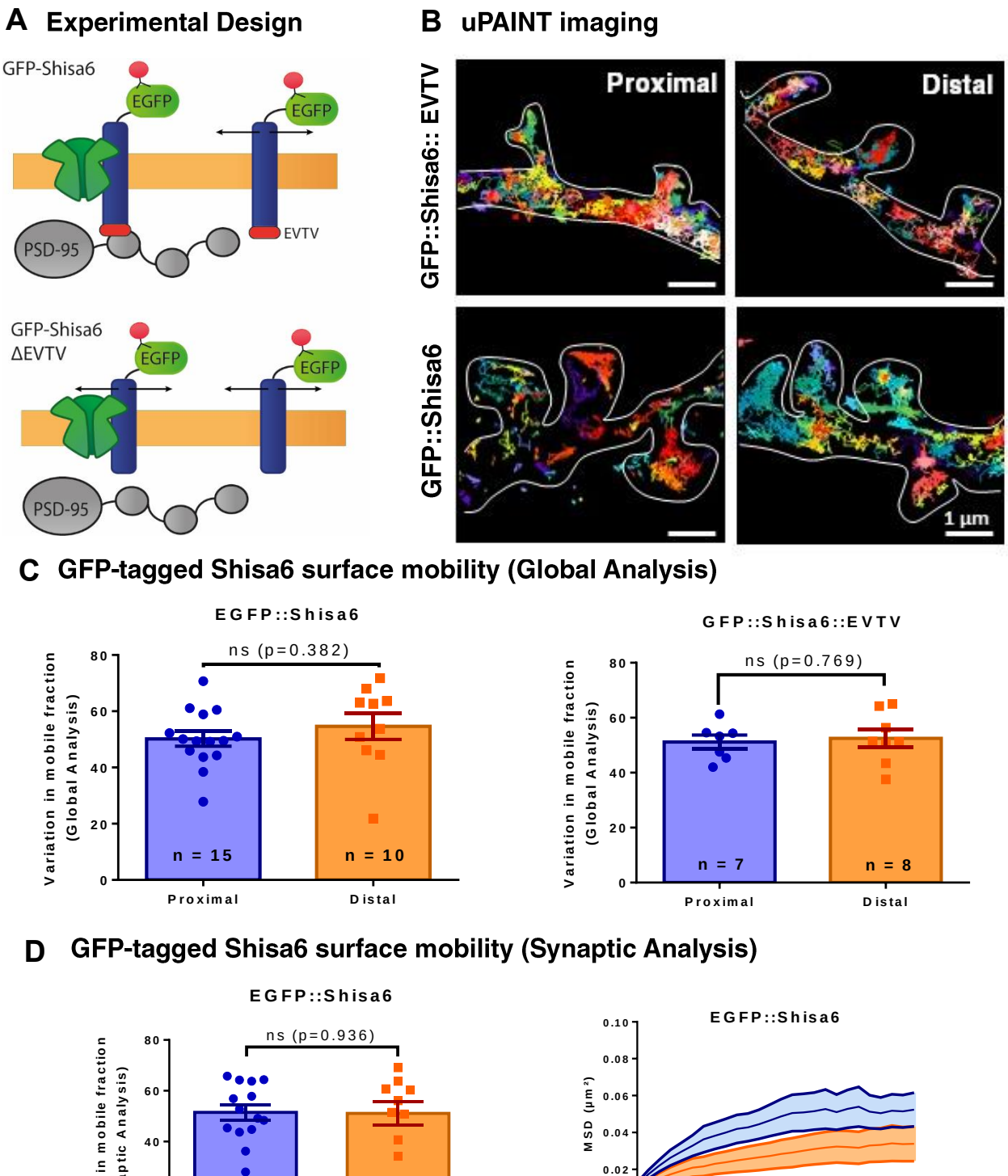

Figure legend in the next page

Figure 13 – Overexpressed GFP::Shisa6 does not shows differences in surface mobility between distal and proximal regions: A) uPAINT microscopy was performed using nanobodies coupled to ATTO647N directed against the extracellular EGFP-tag of the overexpressed Shisa6 and Shisa6 EVTV. **B)** Super-resolved images of overexpressed EGFP-tagged Shisa6 and Shisa6 EVTV. Dendritic and synaptic regions were defined by wavelet segmentation of the EGFP signal for both proximal (50-120 μm) and distal (220 – 290 μm) recordings. **C)** Cumulative variation of the mobile fraction (D> -1.6 μm2/s) for both dendritic and synaptic regions. EGFP::Shisa6: Proximal recordings = 50.2 ± 2.64 (n=15); Distal Recordings = 54.6 ± 4.67 (n=10); unpaired t-test, p=0.382. EGFP::Shisa6::EVTV: Proximal recordings = 51.20 ± 2.49 (n=7); Distal Recordings = 52.47 ± 3.33 (n=8); unpaired t-test, p= 0.769. **D)** *(Left panel)* Cumulative variation inside mobile fraction for synaptic trajectories. EGFP::Shisa6: Proximal recordings = 51.52 ± 3.05 (n=14); Distal Recordings = 51.10 ± 4.52 (n=10); unpaired t-test, p= 0.936. EGFP::Shisa6::EVTV: Proximal recordings = 52.16 ± 3.03 (n=7); Distal Recordings = 52.47 ± 3.45 (n=7); unpaired t-test, p=0.947. *(Right panel)* Graphical representation of MSD curves. EGFP::Shisa6: Proximal recordings MSD plateau= 0.052 ± 0.009 μm^2 at t=0.5s; Distal Recordings MSD plateau = 0.033 ± 0.0094 μm^2 at t=0.5s. EGFP::Shisa6::EVTV: Proximal recordings MSD plateau = 0.0579 ± 0.404 μm^2 at t=0.5s; Distal Recordings MSD plateau = 0.050 ± 0.009 μm^2 at t=0.5s .

Discussion

Discussion

The current study took advantage of a combination of different microcopy techniques to further characterize the relationship between Shisa6 and AMPARs. Wide field microscopy suggested a preferential expression of Shisa6 in distal synaptic regions where it impacts synaptic morphology. This preliminary data raises the possibility that this protein has a synaptic expression gradient. Because Shisa6 is synaptically localized, is interacting with AMPARs and can bind PDZ-containing scaffold elements, it might regulate receptor surface mobility. dSTORM revealed that Shisa6 *KO* does not change receptor nanoscale organization in both proximal and distal synaptic regions. Interestingly, this is not associated with major changes in AMPARs surface expression. uPAINT showed that Shisa6 *KO* does not alter the surface mobility of AMPARs in mice hippocampal neurons. To exclude compensatory mechanism of the global *KO*, uPAINT was performed in rat hippocampal neurons with acute manipulation of the endogenous Shisa6 levels. Notably, Shisa6 EVTV increased AMPAR surface mobility in distal dendritic regions. Altogether these results suggests a complex relationship between Shisa6 and AMPARs. Indeed, Shisa6 is able to regulate AMPAR surface mobility in hippocampal neurons through its interaction with PDZ-domain containing proteins. Likely due to its expression gradient, the effect of Shisa6 is preferential for distal dendrites.

The acute manipulation of Shisa6 had a bidirectional impact in spine morphology development. The developmental alterations of dendritic spine morphology are characterized in primary hippocampal neurons (Papa et al., 1995). The majority of dendritic spine-like structures resembled long filopodia at 7 *DIV*. With increased time in culture, these filopodia-like structures were progressively replaced by mature dendritic spines. In agreement, mushroom-like spines constituted the major spine population at 21 *DIV* (Papa et al., 1995). It is hypothesized that Shisa6 favors spine morphology development. Shisa6 overexpression increased the number of mushroom-like spines at 10-14 *DIV*. This increase is restricted to early developmental stages since no differences are seen at 21 *DIV*. Likewise, the effect of Shisa6 in spine structure might be restricted to a critical window of development. AMPAR surface expression impacts dendritic spine morphology (Krekelberg et al., 2003; Hanley, 2008). DG ganule cells of *Gria2 KO* mice exhibit changes in spine morphology with fewer mushroom spines and more immature thin spines (Medvedev et al., 2008). In parallel, Shisa9 is reported to impact spinogenesis indirectly by regulating the number of AMPARs at the cell membrane (Khodosevich et al., 2014). It is possible that the effect of Shisa6 in spine morphology results from a differential regulation of AMPARs at the cell surface. By increasing the number of surface AMPARs, Shisa6 might facilitate the progress from filopodia-like to mushroom-like spines during early stages of development. Moreover, Shisa6 cannot promote further morphology development at late developmental stages where the population of spines is predominantly mature. Paradoxically, the impairment of spine maturation by Shisa6 *KD* is persistent and independent of the distance to the soma. Even if the impact is

higher for distal dendrites at late developmental stages, this is not consistent with the hypothesized early action of Shisa6. These results may point to a complex differential effect of Shisa6 throughout development that needs to be further explored. Additional work needs to be performed to better understand the relationship between Shisa6 and spine structure. It would be interesting to determine if, similarly to Shisa9, Shisa6 also impacts the number of dendritic spines and the overall dendritic morphology (Khodosevich et al., 2014).

Being expressed throughout the hippocampus, Shisa6 is proposed to sustain synaptic transmission during high frequency stimulation (Klaassen et al., *in revision).* Indeed, synaptic transmission is highly depressed during paired-pulse recordings of Shisa6 *KO* hippocampal CA1 pyramidal neurons. This suggests that Shisa6 is able to regulate synaptic transmission by direct modulation of endogenous AMPARs gating properties. Surprisingly, Shisa6 *KO* did not impact AMPARs surface mobility neither synaptic nano-organization in mice hippocampal neurons. How is possible to conciliate the apparent discrepancy between these structural and electrophysiological studies? This conundrum can be explained by a functional redundancy between different auxiliary proteins associated within the same AMPAR complex. Endogenous AMPARs are described as large macromolecular complexes comprising the association of a large heterogeneity of different auxiliary proteins (Schwenk et al., 2012). The meaning of such complexity is unknown, but the AMPAR-modulatory effect of auxiliary proteins is now appreciated to be additive, complimentary, or functional redundant. It is suspected that the absence of Shisa6 is compensated by a different auxiliary protein, ensuring a synergistic regulation of AMPARs diffusional properties. In the hippocampus, CA1 pyramidal neurons are known to express multiple TARP family members, including stargazin, γ-3, γ-4, γ-7, and γ-8 (Tomita et al., 2003; Fukaya et al., 2005; Lein et al., 2007). Stargazer/γ-3 double *KO* (Menuz et al., 2008) and γ-3/γ-4 double *KO* (Menuz et al., 2009) fail to exhibit an impairment of synaptic transmission in this cell type. This suggests that, at least in CA1 pyramidal neurons, multiple TARPs are redundant, and one TARP can compensate the loss of the others to mediate AMPAR synaptic targeting. Moreover, a recent study revealed that AMPARs expressed in DG granule cells are under regulation of two auxiliary subunits: Shisa9 and TARP γ-8 (Khodosevich et al., 2014). Interestingly, both auxiliary proteins are described to promote AMPAR surface expression, while differentially impacting receptor gating properties (Khodosevich et al., 2014). A distinct modulation by coexpressed auxiliary subunits can justify why Shisa6 *KO* impacts AMPAR gating properties, without affecting receptor nano-organization and surface mobility. Considering the richness of different auxiliary subunits expressed throughout the hippocampus, a functional redundancy to ensure a proper AMPAR function is likely. In agreement, all the TARPs mentioned above present a PDZ ligand-motif that, under basal conditions, can ensure a proper AMPAR synaptic localization (Tomita et al., 2003; Kato et al., 2010). The same stands true regarding AMPAR surface expression (Chen et al., 2000; Tomita et al., 2003). On the other hand, Shisa6 expression can be dynamically changed along the development. It is described that the composition of the AMPAR complex is subjected to a regional, developmental,

and cell-specific regulation. (Schwenk et al., 2014). It would be interesting to explore the exact developmental expression of Shisa6 in our cultures and understand if the interaction with AMPAR occurs in a specific time-window. Another exciting possibility is that the interaction between AMPAR and Shisa6 is dynamically regulated during synaptic activity. It has been reported that, upon binding of glutamate, AMPARs detached from TARPs (Tomita et al., 2004). A recent work from our group showed that this allosteric mechanism increases AMPAR mobility, the exchange of receptors between nanodomains, and allows faster recovery from desensitization-mediated synaptic depression (Constals et al., 2015). Since Shisa6 keeps AMPARs in an activated state during prolonged presence to glutamate, plasticity events might modulate the impact of this protein on receptor lateral diffusion.

The result obtained from overexpression of the Shisa6 EVTV mutant strongly support that Shisa6 is indeed able to regulate AMPAR surface mobility. However, this modulation results from a complex relationship between Shisa6 and AMPARs. Both Shisa6 *KD* and Shisa6 overexpression failed to regulate AMPAR surface mobility. Similarly to Shisa6 *KO*, a redundancy between auxiliary proteins can blunt the increase in AMPAR mobility expected for Shisa6 *KD*. However, the lack of effect of Shisa6 overexpression is more challenging to be drawn. Remarkably, overexpression of Shisa6 EVTV increased AMPAR surface mobility exclusively at distal dendrites. The discrepancy of results between overexpressing a full length form or the EVTV mutant of Shisa6 raises the puzzling possibility that we may be in the presence of a dominant negative effect. Assuming that Shisa6 (1) has a unique binding site in AMPAR; and (2) endogenous expression levels occupies all the available slots, its overexpression will not further increase AMPARs stabilization. Due to the presence of a PDZ ligand-domain in both proteins, the same preposition stands true if Shisa6 binding site is shared with TARPs. Moreover, the effect of Shisa6 EVTV overexpression can be described by a direct displacement of endogenous Shisa6/TARPs from their binding sites. This hypothetical model is in agreement with a distance-dependent action of Shisa6: although Shisa6 EVTV overexpression does not impact AMPAR surface mobility in proximal dendrites, it profoundly changes this property in distal ones. The precise interaction between Shisa6 and AMPAR is currently unknown. Studies exploring the mechanism of binding and the stoichiometry of this interaction will be of decisive importance to understand how Shisa6 regulates AMPAR diffusional properties. It is reported that in DG granule cells, Shisa9 is complexed within TARP γ-8/AMPAR complexes (Khodosevich et al., 2014). On the other hand, in the tripartite complex formed by CNIH2/AMPAR/TARP, CNIH2 and TARPs show a competitive interaction with the AMPAR (Kato et al., 2010; Gill et al., 2011). Determine if Shisa6 has a competitive or a cooperative action with others coexpressed auxiliary subunits will provide valuable information about its function.

Shisa6 EVTV increased AMPAR diffusion and strongly decreases AMPAR stabilization at the synapse. During basal conditions, most AMPARs are constantly alternating between immobile and mobile states driven by lateral diffusion (Borgdorff and Choquet, 2002; Bats et al., 2007). AMPAR

stabilization at the synapse involves the interaction of auxiliary subunits with intracellular scaffolding proteins. A canonical example of such interaction is the activity-dependent stabilization of AMPARs through binding of the PDZ ligand-binding motif of stargazin to PSD-95 (Bats et al., 2007). The reversible binding between stargazin and PSD-95 drives AMPARs between diffusive and immobilize states. Here, using a Shisa6 EVTV mutant, we report that the effect of Shisa6 in AMPAR surface mobility is also dependent on interactions between its PDZ ligand-binding motif and scaffolding proteins. If Shisa6 and TARPs act synergistically or competitively to control AMPAR synaptic stabilization remains to be determined.

Signal propagation through dendrites is subjected to distance-dependent filtering and attenuation, potentially limiting the influence of distal synapses in somatic integration (Rall 1977). To counteract this situation, neurons adjust the strength of individual synapses to make them equally able to impact the information output independently of their distance to the soma (Magee and Cook, 2000). This distance-dependent scaling is proposed to require an increase of synaptic AMPARs in distal synaptic sites (Andrásfalvy and Magee, 2001; Nicholson et al., 2006). Bearing in mind the heterogeneity at the single-synapse level, it is likely that both proximal and distal synapses have a different molecular composition (Micheva et al., 2010; Collman et al., 2015). This heterogeneity would endow neurons with the molecular machinery required to ensure a proper topological regulation of AMPARs. Due to its synaptic expression gradient, Shisa6 fills the requirement for such regulation. Indeed, different evidences led us to suggest a distance-dependent action of Shisa6: (1) EGFP::Shisa6 was preferentially accumulated in distal synaptic sites; (2) Shisa6 overexpression impacted synaptic morphology in distal dendrites; (3) Shisa6 EVTV selectively increased AMPAR mobility in this region. This is in agreement with a preferential role of Shisa6 for distal synapses, where is able to regulate AMPARs surface mobility. How do we foresee this functional compartmentalization? An appealing possibility is an interaction between Shisa6 and a scaffolding element preferentially accumulated in distal dendrites. Shisa9 is reported to be able to interact with different PDZ domain-containing interactors (Karataeva et al., 2014). Shisa-like proteins have only one PDZ ligand-binding motif, indicating that the interaction with their partners has to be strictly regulated and that may possibly vary between synapses or intracellular compartments. It is possible that the PDZ ligand-binding of Shisa6 interacts with different intracellular partners to ensure an accumulation in distal dendrites. As a consequence, the effect of Shisa6 in AMPAR surface mobility would be restricted to these regions. This is supported by the results obtained on GluA2 surface mobility when overexpressing Shsia6 EVTV mutant. The hypothesis of a distance-dependent regulation of AMPAR surface mobility requires experimental validation, it is however a very appealing concept which would bring a new level of regulation of glutamate receptors, and deeply impact our current knowledge of synaptic plasticity mechanisms.

Conclusion and further perspectives

Conclusion and future perspectives

In this study we have characterized a role for Shisa6 in AMPAR surface mobility. By anchoring AMPARs to scaffolding elements, auxiliary proteins regulate the interplay between lateral diffusion and synaptic trapping. Essential to organize receptors at the synapse, auxiliary subunits are now considered the major determinants of AMPAR dynamic molecular organization. This structural organization has direct implications in both the properties and efficacy of synaptic function. Moreover, exploring the composition of the AMPAR complex is essential to better understand the complex mechanisms used by neurons to regulate synaptic transmission during basal condition or in response to activity. Despite the recent characterization of a large number of auxiliary subunits, the physiological meaning of such complexity is still an open question. By describing Shisa6 role in AMPAR surface mobility, the present work made a decisive contribution in this direction. To our knowledge, this is the first study to report a distance-dependent mechanism for an AMPAR auxiliary protein. This study will further enlarge the synaptic diversity at the single-neuron level, and the amount of regulation points for synaptic properties adjustments. Our results expose yet another layer of complexity, making clear that we are just beginning to appreciate the functional diversity of AMPAR auxiliary proteins

We have suggested a distance-dependent effect of Shisa6 in AMPAR surface mobility. To further describe this compartmentalization, a combination of structural and functional studies is required. dSTORM can be applied to determine if EGFP::Shisa6 has a differential surface expression between proximal and distal dendrites. Moreover, addressing the nanoscale organization of EGFP::Shisa6 and GluA2-containing AMPARs will confirm Shisa6 distance-dependent effect. To further corroborate the information obtained with this imaging techniques, an electrophysiological approach can be considered. Acute manipulation of synaptic AMPARs with 2-Photon glutamate uncaging can be a valuable tool to address differences in Shisa6 function between proximal and distal dendrites. By recording synaptic AMPARs currents, at single-synapse level, in a Shisa6 *KO* background, will provide valuable information about a functional compartmentalization of Shisa6.

Shisa6 *KO* did not impact AMPAR surface mobility neither nano-organization. We proposed that this lack of effects is due a functional redundancy between different AMPAR auxiliary proteins. Is thus possible that Shisa6 *KO* induces the upregulation of another auxiliary subunit expressed in our experimental conditions. Western blot should be performed to determine the expression levels of (1) different TARPs (e.g., stargazin) and (2) different AMPAR subunits and PSD-95. This approach would clarify some of the results here obtained with dSTORM. Lastly, Shisa6 *KO* can also be used to further explore the impact of Shisa6 in spine morphology by analyzing spine morphology and the ratio of spinogenesis.

Evidences for a role of Shisa6 in AMPAR surface mobility were obtained with the acute manipulation of this protein. Furthermore, a similar approach could be extended to dSTORM experiments in order to determine if the reported effect in AMPAR mobility is translated in alterations at the nanoscale level. This would potentially overcome the compensatory mechanisms

induced by Shisa6 *KO* and would allow to determine if Shisa6 impacts synaptic nanodomains organization. We hypothesized that, similar to Shisa9, Shisa6 impacts spine morphology by a differential regulation of AMPARs surface expression. Although our analysis did not detect an effect of Shisa6 overexpression or downregulation on the number of AMPARs, it would be interesting to evaluate the expression of this receptor at the cell surface, by purification of biotinylated protein fraction for example. By defining the role of Shisa6 in targeting AMPAR to the cell membrane, this approach would allow to test our hypothesis about their impact in spine morphology development.

The effect of Shisa6 in AMPAR surface mobility appears to depend on interactions between its PDZ ligand-binding motif and scaffolding proteins (e.g., PSD-95). Similarly to TARPs, this interaction can be regulated by neuronal activity due to posttranslational modifications. It could be of outstanding interest not only to determine the specific interactors of this protein, but also if Shisa6 CTD contains conserved phosphorylation sites substrate for CaMKII and/or PKC regulation. To determine if the phosphorylation state of Shisa6 modulates its interaction with intracellular partners, a co-IP experiments can be performed. Using heterologous cells transfected with different Shisa6 phosphomutants and PSD-95 can give important information about how neuronal activity might regulate this interaction. Finally, uPAINT can be applied to determine if the different phosphomutants have a different impact in AMPAR surface mobility. To link this regulation to differential interaction with PSD-95, a FLIM-FRET study between the different can be considered.

Shisa6 is crucial to sustain synaptic transmission during high frequency stimulation. This led us to hypothesize that the effect of this auxiliary subunit in AMPAR surface mobility can be dramatically changed by neuronal activity. The next step to further explore this possibility is to couple different super-resolution microscopy techniques with chemical-induced LTP or LTD protocols. Using Shisa6 *KO* hippocampal neurons, this simple approach will inform about the importance of Shisa6 in AMPAR organization during this forms of plasticity. This should be complemented with electrophysiological studies to determine if Shisa6 *KO* have any impairments in the induction of this forms of plasticity. Another remarkably possibility is that the effect of Shisa6 in AMPAR surface mobility depends on receptor conformational state. Recent work proposed that bath glutamate application increases AMPAR mobility due to the unbinding from stargazin (Constals et al., 2015). Considering the effect of Shisa6 in AMPAR desensitization, can be interesting to determine its role during the reported glutamate effect. As a first screening, uPAINT can be applied to understand if this increase in AMPAR mobility is still present in Shisa6 *KO* mice hippocampal neurons. To corroborate if Shisa6/AMPAR relationship is modulated by receptor desensitization, we can make usage of different GluA2 mutants locked in different conformation states. By coexpressing these different mutants with EGFP::Shisa6 in heterologous cells, we can perform co-IP experiments to measure their interaction.

In this study we have shown that it is possible to use multiple super-resolution top-of-the-edge microscopy techniques to explore in detail synapse composition and the mechanisms of its regulation. Understanding the fine modulation of AMPARs surface mobility is crucial to comprehend its contribution to the adjustments of synaptic strength, which has implicated not only in mechanisms of learning and memory but also in several neurological disorders.

Bibliography

Andrásfalvy BK, Magee JC (2001) Distance-dependent Increase in AMPA Receptor Number in the Dendrites of Adul Hippocampal CA1 Pyramidal Neurons. The Journal of Neurosciecne 21:9151-9159.

Anggono V, Huganir RL (2012) Regulation of AMPA receptor trafficking and synaptic plasticity. Curr Opin Neurobiol 22:461-469.

Armstrong N, Gouaux E (2000) Mechanisms for activation and antagonism of an AMPA-sensitive glutamate receptor: crystal structures of the GluR2 ligand binding core. Neuron 28:165-181.

Bats C, Groc L, Choquet D (2007) The interaction between Stargazin and PSD-95 regulates AMPA receptor surface trafficking. Neuron 53:719-734.

Bhatt DH, Zhang S, Gan WB (2009) Dendritic spine dynamics. Annu Rev Physiol 71:261-282.

Bliss TVP, Collingridge GL (1993) A synaptic model of memory: long-term potentation in the hippocampus. Nature 361:31-39.

Borgdorff AJ, Choquet D (2002) Regulation of AMPA receptor lateral movements. Nature 417:649-653.

Brockie PJ, Jensen M, Mellem JE, Jensen E, Yamasaki T, Wang R, Maxfield D, Thacker C, Hoerndli F, Dunn PJ, Tomita S, Madsen DM, Maricq AV (2013) Cornichons control ER export of AMPA receptors to regulate synaptic excitability. Neuron 80:129-142.

Calabrese B, Wilson MS, Halpain S (2006) Development and regulation of dendritic spine synapses. Physiology (Bethesda) 21:38-47.

Carroll RC, Lissin DV, von Zastrow M, Nicoll RA, Malenka RC (1999) Rapid redistribution of glutamate receptors contributes to long-term depression in hippocampal cultures. Nat Neurosci 2:454-460.

Chen L, Chetkovich DM, Petralia RS, Sweeney NT, Kawasaki Y, Wenthold RJ, Bredt DS, Nicoll RA (2000) Stargazin regulates synaptic targeting of AMPA receptors by two distinct mechanisms. Nature 408:936-943.

Cho KO, Hunt CA, Kennedy MB (1992) The rat brain postsynaptic density fraction contains a homolog of the Drosophila discs-large tumor suppressor protein. Neuron 9:929-942.

Choquet D (2010) Fast AMPAR trafficking for a high-frequency synaptic transmission. Eur J Neurosci 32:250-260.

Choquet D, Triller A (2013) The dynamic synapse. Neuron 80:691-703.

Cognet L, Leduc C, Lounis B (2014) Advances in live-cell single-particle tracking and dynamic super-resolution imaging. Curr Opin Chem Biol 20:78-85.

Collingridge GL, Isaac JT, Wang YT (2004) Receptor trafficking and synaptic plasticity. Nat Rev Neurosci 5:952-962.

Collingridge GL, Olsen RW, Peters J, Spedding M (2009) A nomenclature for ligand-gated ion channels. Neuropharmacology 56:2-5.

Collman F, Buchanan J, Phend KD, Micheva KD, Weinberg RJ, Smith SJ (2015) Mapping synapses by conjugate light-electron array tomography. J Neurosci 35:5792-5807.

Colquhoun D, Jonas P, Sakmann B (1992) Action of brief pulses of glutamate on AMPA/Kainate Receptors in patches from different neurons of rat hippocampal slices. The Journal of Physiology 458:261-287.

Constals A, Penn AC, Compans B, Toulme E, Phillipat A, Marais S, Retailleau N, Hafner AS, Coussen F, Hosy E, Choquet D (2015) Glutamate-induced AMPA receptor desensitization increases their mobility and modulates short-term plasticity through unbinding from Stargazin. Neuron 85:787-803.

Ehlers MD (2000) Reinsertion or degradation of AMPA receptors determined by activity-dependent endocytic sorting. Neuron 28:511-525.

Ehlers MD (2013) Dendritic trafficking for neuronal growth and plasticity. Biochem Soc Trans 41:1365-1382.

Ehrlich I, Malinow R (2004) Postsynaptic density 95 controls AMPA receptor incorporation during long-term potentiation and experience-driven synaptic plasticity. J Neurosci 24:916-927.

Frischknecht R, Heine M, Perrais D, Seidenbecher CI, Choquet D, Gundelfinger ED (2009) Brain extracellular matrix affects AMPA receptor lateral mobility and short-term synaptic plasticity. Nat Neurosci 12:897-904.

Fukata Y, Dimitrov A, Boncompain G, Vielemeyer O, Perez F, Fukata M (2013) Local palmitoylation cycles define activity-regulated postsynaptic subdomains. J Cell Biol 202:145-161.

Fukaya M, Yamazaki M, Sakimura K, Watanabe M (2005) Spatial diversity in gene expression for VDCCgamma subunit family in developing and adult mouse brains. Neurosci Res 53:376-383.

Giannone G, Hosy E, Levet F, Constals A, Schulze K, Sobolevsky AI, Rosconi MP, Gouaux E, Tampe R, Choquet D, Cognet L (2010) Dynamic superresolution imaging of endogenous proteins on living cells at ultra-high density. Biophys J 99:1303-1310.

Gill MB, Kato AS, Roberts MF, Yu H, Wang H, Tomita S, Bredt DS (2011) Cornichon-2 modulates AMPA receptor-transmembrane AMPA receptor regulatory protein assembly to dictate gating and pharmacology. J Neurosci 31:6928-6938.

Greger IH, Ziff EB, Penn AC (2007) Molecular determinants of AMPA receptor subunit assembly. Trends Neurosci 30:407-416.

Hafner AS, Penn AC, Grillo-Bosch D, Retailleau N, Poujol C, Philippat A, Coussen F, Sainlos M, Opazo P, Choquet D (2015) Lengthening of the Stargazin Cytoplasmic Tail Increases Synaptic Transmission by Promoting Interaction to Deeper Domains of PSD-95. Neuron 86:475-489.

Hanley JG (2008) AMPA receptor trafficking pathways and links to dendritic spine morphogenesis. Cell Adh Migr 2:276-282.

Harmel N, Cokic B, Zolles G, Berkefeld H, Mauric V, Fakler B, Stein V, Klocker N (2012) AMPA receptors commandeer an ancient cargo exporter for use as an auxiliary subunit for signaling. PLoS One 7:e30681.

Heine M, Groc L, Frischknecht R, Beique JC, Lounis B, Rumbaugh G, Huganir RL, Cognet L, Choquet D (2008) Surface mobility of postsynaptic AMPARs tunes synaptic transmission. Science 320:201-205.

Hering H, Sheng M (2001) Dendritic spines: structure, dynamics and regulation. Nat Rev Neurosci 2:880-888.

Herring BE, Shi Y, Suh YH, Zheng CY, Blankenship SM, Roche KW, Nicoll RA (2013) Cornichon proteins determine the subunit composition of synaptic AMPA receptors. Neuron 77:1083-1096.

Ho VM, Lee JA, Martin KC (2011) The cell biology of synaptic plasticity. Science 334:623-628.

Huganir RL, Nicoll RA (2013) AMPARs and synaptic plasticity: the last 25 years. Neuron 80:704-717.

Jackson AC, Nicoll RA (2011) The expanding social network of ionotropic glutamate receptors: TARPs and other transmembrane auxiliary subunits. Neuron 70:178-199.

Jiang J, Suppiramaniam V, Wooten MW (2006) Posttranslational modifications and receptor-associated proteins in AMPA receptor trafficking and synaptic plasticity. Neurosignals 15:266-282.

Jones MV, Westbrook GL (1996) The impact of receptor desensitization on fast synaptic transmission. Trends Neurosci 19:96-101.

Kaech S, Banker G (2006) Culturing hippocampal neurons. Nat Protoc 1:2406-2415.

Kalashnikova E, Lorca RA, Kaur I, Barisone GA, Li B, Ishimaru T, Trimmer JS, Mohapatra DP, Diaz E (2010) SynDIG1: an activity-regulated, AMPA- receptor-interacting transmembrane protein that regulates excitatory synapse development. Neuron 65:80-93.

Karataeva AR, Klaassen RV, Stroder J, Ruiperez-Alonso M, Hjorth JJ, van Nierop P, Spijker S, Mansvelder HD, Smit AB (2014) C-terminal interactors of the AMPA receptor auxiliary subunit Shisa9. PLoS One 9:e87360.

Kato AS, Gill MB, Ho MT, Yu H, Tu Y, Siuda ER, Wang H, Qian YW, Nisenbaum ES, Tomita S, Bredt DS (2010) Hippocampal AMPA receptor gating controlled by both TARP and cornichon proteins. Neuron 68:1082-1096.

Kennedy MJ, Davison IG, Robinson CG, Ehlers MD (2010) Syntaxin-4 defines a domain for activity-dependent exocytosis in dendritic spines. Cell 141:524-535.

Khodosevich K, Jacobi E, Farrow P, Schulmann A, Rusu A, Zhang L, Sprengel R, Monyer H, von Engelhardt J (2014) Coexpressed auxiliary subunits exhibit distinct modulatory profiles on AMPA receptor function. Neuron 83:601-615.

Klaassen, R.V., Stroeder, J., Coussen, F., Hafner, A.S., Petersen, J.D., Renancio, C., Lodder, J.C., Rotaru, D.C., Schmitz, L.J.M., Rao-Ruiz, P., Spijker, S., Huibert D. Mansvelder, H.D. Choquet, D. and Smit, A.B. Shisa6 traps AMPARs at postsynaptic sites and prevents their desensitization during high frequency synaptic stimulation. In revision at Nature Neuroscience.

Kim E, Sheng M (2004) PDZ domain proteins of synapses. Nat Rev Neurosci 5:771-781.

Krekelberg B, Dannenberg S, Hoffmann KP, Bremmer F, Ross J (2003) Neural correlates of implied motion. Nature 424:674-677.

Lamprecht R, LeDoux J (2004) Structural plasticity and memory. Nat Rev Neurosci 5:45-54.

Lee SH, Simonetta A, Sheng M (2004) Subunit rules governing the sorting of internalized AMPA receptors in hippocampal neurons. Neuron 43:221-236.

Lein ES et al. (2007) Genome-wide atlas of gene expression in the adult mouse brain. Nature 445:168-176.

Lerma J, Marques JM (2013) Kainate receptors in health and disease. Neuron 80:292-311.

Letts VA, Felix R, Biddlecome GH, Arikkath J, Mahaffey CL, Valenzuela A, Bartlett FS, 2nd, Mori Y, Campbell KP, Frankel WN (1998) The mouse stargazer gene encodes a neuronal Ca2+-channel gamma subunit. Nat Genet 19:340-347.

Li Z, Sheng M (2003) Some assembly required: the development of neuronal synapses. Nat Rev Mol Cell Biol 4:833-841.

Lisman J, Raghavachari S (2006) A unified model of the presynaptic and postsynaptic changes during LTP at CA1 synapses. Sci STKE 2006:re11.

Liu SJ, Zukin RS (2007) Ca2+-permeable AMPA receptors in synaptic plasticity and neuronal death. Trends Neurosci 30:126-134.

Lledo PM, Zhang X, Sudhof TC, Malenka RC, Nicoll RA (1998) Postsynaptic membrane fusion and long-term potentiation. Science 279:399-403.

Lomeli H, Sprengel R, Laurie DJ, Kohr G, Herb A, Seeburg PH, Wisden W (1993) The rat delta-1 and delta-2 subunits extend the excitatory amino acid receptor family. FEBS Lett 315:318-322.

Louros SR, Hooks BM, Litvina L, Carvalho AL, Chen C (2014) A role for stargazin in experience-dependent plasticity. Cell Rep 7:1614-1625.

Lu J, Helton TD, Blanpied TA, Racz B, Newpher TM, Weinberg RJ, Ehlers MD (2007) Postsynaptic positioning of endocytic zones and AMPA receptor cycling by physical coupling of dynamin-3 to Homer. Neuron 55:874-889.

Lu W, Shi Y, Jackson AC, Bjorgan K, During MJ, Sprengel R, Seeburg PH, Nicoll RA (2009) Subunit composition of synaptic AMPA receptors revealed by a single-cell genetic approach. Neuron 62:254-268.

Luscher C, Malenka RC (2012) NMDA receptor-dependent long-term potentiation and long-term depression (LTP/LTD). Cold Spring Harb Perspect Biol 4.

MacGillavry HD, Song Y, Raghavachari S, Blanpied TA (2013) Nanoscale scaffolding domains within the postsynaptic density concentrate synaptic AMPA receptors. Neuron 78:615-622.

Magee JC, Cook EP (2000) Somatic EPSP amplitude is independent of synaptic location in hippocampal pyramidal neurons. Nat Neurosci 3:859-903.

Makino H, Malinow R (2009) AMPA receptor incorporation into synapses during LTP: the role of lateral movement and exocytosis. Neuron 64:381-390.

Medvedev NI, Rodriguez-Arellano JJ, Popov VI, Davies HA, Tigaret CM, Schoepfer R, Stewart MG (2008) The glutamate receptor 2 subunit controls post-synaptic density complexity and spine shape in the dentate gyrus. Eur J Neurosci 27:315-325.

Meldrum BS (2000) Glutamate as a Neurotransmitter in the Brain: Review of Physiology

and Pathology. Journal of Nutrition 130:1007-1015.

Menuz K, Kerchner GA, O'Brien JL, Nicoll RA (2009) Critical role for TARPs in early development despite broad functional redundancy. Neuropharmacology 56:22-29.

Menuz K, O'Brien JL, Karmizadegan S, Bredt DS, Nicoll RA (2008) TARP redundancy is critical for maintaining AMPA receptor function. J Neurosci 28:8740-8746.

Micheva KD, Busse B, Weiler NC, O'Rourke N, Smith SJ (2010) Single-synapse analysis of a diverse synapse population: proteomic imaging methods and markers. Neuron 68:639-653.

Milstein AD, Nicoll RA (2008) Regulation of AMPA receptor gating and pharmacology by TARP auxiliary subunits. Trends Pharmacol Sci 29:333-339.

Nair D, Hosy E, Petersen JD, Constals A, Giannone G, Choquet D, Sibarita JB (2013) Super-resolution imaging reveals that AMPA receptors inside synapses are dynamically organized in nanodomains regulated by PSD95. J Neurosci 33:13204-13224.

Nicholson DA, Trana R, Katz Y, Kath WL, Spruston N, Geinisman Y (2006) Distance-dependent differences in synapse number and AMPA receptor expression in hippocampal CA1 pyramidal neurons. Neuron 50:431-442.

Nicoll RA, Bredt DS (2003) AMPA Receptor Trafficking at Excitatory Synapses. Neuron 40:361-379.

Nimchinsky EA, Sabatini BL, Svoboda K (2002) Structure and function of dendritic spines. Annu Rev Physiol 64:313-353.

Niswender CM, Conn PJ (2010) Metabotropic glutamate receptors: physiology, pharmacology, and disease. Annu Rev Pharmacol Toxicol 50:295-322.

Opazo P, Choquet D (2011) A three-step model for the synaptic recruitment of AMPA receptors. Mol Cell Neurosci 46:1-8.

Opazo P, Labrecque S, Tigaret CM, Frouin A, Wiseman PW, De Koninck P, Choquet D (2010) CaMKII triggers the diffusional trapping of surface AMPARs through phosphorylation of stargazin. Neuron 67:239-252.

Paoletti P, Neyton J (2007) NMDA receptor subunits: function and pharmacology. Curr Opin Pharmacol 7:39-47.

Papa M, Bundman VG, Segal M (1995) Morphological Analysis of Ddendritc Spine Development in Primary Cultures of Hippocampal Neurons. The Journal of Neurosciecne 15:1-11.

Park M, Salgado JM, Ostroff L, Helton TD, Robinson CG, Harris KM, Ehlers MD (2006) Plasticity-induced growth of dendritic spines by exocytic trafficking from recycling endosomes. Neuron 52:817-830.

Pei J, Grishin NV (2012) Unexpected diversity in Shisa-like proteins suggests the importance of their roles as transmembrane adaptors. Cell Signal 24:758-769.

Portera-Cailliau C, Pan DT, Yuste R (2003) Activity-regulated dynamic behavior of early dendritic protrusions: evidence for different types of dendritic filopodia. J Neurosci 23:7129-7142.

Preibisch S, Saalfeld S, Tomancak P (2009) Globally optimal stitching of tiled 3D microscopic image acquisitions. Bioinformatics 25:1463-1465.

Priel A, Kolleker A, Ayalon G, Gillor M, Osten P, Stern-Bach Y (2005) Stargazin reduces desensitization and slows deactivation of the AMPA-type glutamate receptors. J Neurosci 25:2682-2686.

Racz B, Blanpied TA, Ehlers MD, Weinberg RJ (2004) Lateral organization of endocytic machinery in dendritic spines. Nat Neurosci 7:917-918.

Rall, W. (2007) Core conductor theory and cable properties of neurons. In Handbook of Physiology. The Nervous System. Cellular Biology of Neurons, E.R. Kandel, J.M. Brookhart, and V.B. Mountcastle, eds. (Bethesda:American Physiological Society), pp. 39–97.

Robert A, Howe JR (2003) How AMPA Receptor Desensitization Depends on Receptor Occupancy. The Journal of Neurosciecne 23:847-858.

Rodríguez-Moreno A, Lerma J (1998) Kainate Receptor Modulation of GABA Release Involves a Metabotropic Function. Neuron 20:1211-1218.

Rouach N, Byrd K, Petralia RS, Elias GM, Adesnik H, Tomita S, Karimzadegan S, Kealey C, Bredt DS, Nicoll RA (2005) TARP gamma-8 controls hippocampal AMPA receptor number, distribution and synaptic plasticity. Nat Neurosci 8:1525-1533.

Sainlos M, Tigaret C, Poujol C, Olivier NB, Bard L, Breillat C, Thiolon K, Choquet D, Imperiali B (2011) Biomimetic divalent ligands for the acute disruption of synaptic AMPAR stabilization. Nat Chem Biol 7:81-91.

Santos SD, Carvalho AL, Caldeira MV, Duarte CB (2009) Regulation of AMPA receptors and synaptic plasticity. Neuroscience 158:105-125.

Schwenk J, Baehrens D, Haupt A, Bildl W, Boudkkazi S, Roeper J, Fakler B, Schulte U (2014) Regional diversity and developmental dynamics of the AMPA-receptor proteome in the mammalian brain. Neuron 84:41-54.

Schwenk J, Harmel N, Zolles G, Wolfgang B, Kulik A, Heimrich B, Chisaka O, Jonas P, Schulte U, Fakler B, Klocker N (2009) Functional proteomics identify Cornichon proteins as auxiliary subunits of AMPA receptors. Science 323:1313-1319.

Schwenk J, Harmel N, Brechet A, Zolles G, Berkefeld H, Muller CS, Bildl W, Baehrens D, Huber B, Kulik A, Klocker N, Schulte U, Fakler B (2012) High-resolution proteomics unravel architecture and molecular diversity of native AMPA receptor complexes. Neuron 74:621-633.

Shanks NF, Maruo T, Farina AN, Ellisman MH, Nakagawa T (2010) Contribution of the global subunit structure and stargazin on the maturation of AMPA receptors. J Neurosci 30:2728-2740.

Shanks NF, Savas JN, Maruo T, Cais O, Hirao A, Oe S, Ghosh A, Noda Y, Greger IH, Yates JR, 3rd, Nakagawa T (2012) Differences in AMPA and kainate receptor interactomes facilitate identification of AMPA receptor auxiliary subunit GSG1L. Cell Rep 1:590-598.

Sheng M, Hoogenraad CC (2007) The postsynaptic architecture of excitatory synapses: a more quantitative view. Annu Rev Biochem 76:823-847.

Sheng M, Kim E (2011) The postsynaptic organization of synapses. Cold Spring Harb Perspect Biol 3.

Shepherd JD, Huganir RL (2007) The cell biology of synaptic plasticity: AMPA receptor trafficking. Annu Rev Cell Dev Biol 23:613-643.

Shipman SL, Herring BE, Suh YH, Roche KW, Nicoll RA (2013) Distance-dependent scaling of AMPARs is cell-autonomous and GluA2 dependent. J Neurosci 33:13312-13319.

Sibarita JB (2014) High-density single-particle tracking: quantifying molecule organization and dynamics at the nanoscale. Histochem Cell Biol 141:587-595.

Sobolevsky AI, Rosconi MP, Gouaux E (2009) X-ray structure, symmetry and mechanism of an AMPA-subtype glutamate receptor. Nature 462:745-756.

Sommer B, Keinanen K, Verdoorn TA, Wisden W, Burnashev N, Herb A, Kohler M, Takagi T, Sakmann B, Seeburg PH (1990) Flip and flop: a cell-specific functional switch in glutamate-operated channels of the CNS. Science 249:1580-1585.

Sumioka A (2013) Auxiliary subunits provide new insights into regulation of AMPA receptor trafficking. J Biochem 153:331-337.

Sumioka A, Yan D, Tomita S (2010) TARP phosphorylation regulates synaptic AMPA receptors through lipid bilayers. Neuron 66:755-767.

Tardin C, Cognet L, Bats C, Lounis B, Choquet D (2003) Direct imaging of lateral movements of AMPA receptors inside synapses. EMBO J 22:4656-4665.

Tomita S, Fukata M, Nicoll RA, Bredt DS (2004) Dynamic Interaction of Stargazin-like TARPs with Cycling AMPA receptors at Synapses. Science 303:1508-1511.

Tomita S, Stein V, Stocker TJ, Nicoll RA, Bredt DS (2005a) Bidirectional synaptic plasticity regulated by phosphorylation of stargazin-like TARPs. Neuron 45:269-277.

Tomita S, Chen L, Kawasaki Y, Petralia RS, Wenthold RJ, Nicoll RA, Bredt DS (2003) Functional studies and distribution define a family of transmembrane AMPA receptor regulatory proteins. J Cell Biol 161:805-816.

Tomita S, Adesnik H, Sekiguchi M, Zhang W, Wada K, Howe JR, Nicoll RA, Bredt DS (2005b) Stargazin modulates AMPA receptor gating and trafficking by distinct domains. Nature 435:1052-1058.

Traynelis SF, Wollmuth LP, McBain CJ, Menniti FS, Vance KM, Ogden KK, Hansen KB, Yuan H, Myers SJ, Dingledine R (2010) Glutamate receptor ion channels: structure, regulation, and function. Pharmacol Rev 62:405-496.

Triller A, Choquet D (2008) New concepts in synaptic biology derived from single-molecule imaging. Neuron 59:359-374.

Turetsky D, Garringer E, Patneau DK (2005) Stargazin modulates native AMPA receptor functional properties by two distinct mechanisms. J Neurosci 25:7438-7448.

van de Linde S, Loschberger A, Klein T, Heidbreder M, Wolter S, Heilemann M, Sauer M (2011) Direct stochastic optical reconstruction microscopy with standard fluorescent probes. Nat Protoc 6:991-1009.

Vandenberghe W, Nicoll RA, Bredt DS (2005) Interaction with the unfolded protein response reveals a role for stargazin in biosynthetic AMPA receptor transport. J Neurosci 25:1095-1102.

von Engelhardt J, Mack V, Sprengel R, Kavenstock N, Li KW, Stern-Bach Y, Smit AB, Seeburg PH, Monyer H (2010) CKAMP44: a brain-specific protein attenuating short-term synaptic plasticity in the dentate gyrus. Science 327:1518-1522.

Walker CS, Francis MM, Brockie PJ, Madsen DM, Zheng Y, Maricq AV (2006) Conserved SOL-1 proteins regulate ionotropic glutamate receptor desensitization. Proc Natl Acad Sci U S A 103:10787-10792.

Wang R, Mellem JE, Jensen M, Brockie PJ, Walker CS, Hoerndli FJ, Hauth L, Madsen DM, Maricq AV (2012) The SOL-2/Neto auxiliary protein modulates the function of AMPA-subtype ionotropic glutamate receptors. Neuron 75:838-850.

Wenthold RJ, Petralia RS, Niedzielski AS (1996) Evidence for multiple AMPA receptor complexes in hippocampal CA1/CA2 neurons. The Journal of Neurosciecne 16:1982-1989.

Xiao MY, Zhou Q, Nicoll RA (2001) Metabotropic glutamate receptor activation causes a rapid redistribution of AMPA receptors. Neuropharmacology 41:664-671.

Xu-Friedman MA, Regehr WG (2004) Structural contributions to short-term synaptic plasticity. Physiol Rev 84:69-85.

Xu W (2011) PSD-95-like membrane associated guanylate kinases (PSD-MAGUKs) and synaptic plasticity. Curr Opin Neurobiol 21:306-312.

Yan D, Tomita S (2012) Defined criteria for auxiliary subunits of glutamate receptors. J Physiol 590:21-31.

Yang S-N, Tang Y-G, Zucker RS (1999) Selective Induction of LTP and LTD by postsynaptic [Ca2+] elevation. Journal of Neurophysiology 81:781-787.

Yudowski GA, Puthenveedu MA, Leonoudakis D, Panicker S, Thorn KS, Beattie EC, von Zastrow M (2007) Real-time imaging of discrete exocytic events mediating surface delivery of AMPA receptors. J Neurosci 27:11112-11121.